Exploring the Role of Adaptation and Acclimation in the Temperature Response of Photosynthesis and Respiration in Southern Pine Species

by

Katelyn McBride

A thesis submitted to the Graduate Faculty of
Auburn University
in partial fulfillment of the
requirements for the Degree of
Master of Science

Auburn, Alabama
August 5, 2023

Keywords: Photosynthesis, Respiration, Adaptation, Acclimation, Climate Change

Approved by

Heather D. Alexander, Co-Chair, Associate Professor of Forestry
Michael J. Aspinwall, Co-Chair, Assistant Professor of Forestry
Scott Enebak, Associate Dean and Professor of Forestry

Abstract

Southern pines provide critical ecosystem services, including supplying the global timber market and playing a major role in regional carbon cycling. Yet, many basic knowledge gaps regarding southern pine physiology remain, including the role of temperature adaptation and acclimation on two major physiological processes related to growth and carbon storage: photosynthesis and respiration. Therefore, we conducted a common garden experiment with three or more geographically distinct populations of loblolly (*Pinus taeda*), longleaf (*Pinus palustris*), shortleaf (*Pinus echinata*) and slash pine (*Pinus elliottii*). While species demonstrated significant evidence of respiratory adaptation, there was no evidence of species-level photosynthetic adaptation. Additionally, we found that all species demonstrated evidence of photosynthetic and respiratory acclimation, although the mechanism of acclimation varied between species and populations. Quantifying the temperature responses of photosynthesis and respiration in southern pine species can inform models of carbon fluxes and forest-atmosphere interactions in a future shaped by climate change.

Acknowledgements

This thesis would not have been possible without the many people and organizations who supported it. I would like to thank Dr. Heather Alexander for her time, dedication, and willingness to serve as my advisor. Her edits and insights were critical to the success of this project. I would also like to thank Dr. Michael Aspinwall for providing his expertise and guidance throughout the planning, measurement, analysis, and writing process, as well as for training me on all of the machines and technical skills required for this project. I am deeply indebted to Dr. Jeff Chieppa for his expert statistical and coding guidance, to Dr. Caren Mendonça for her assistance in troubleshooting the Li-6800s, and to Dr. Todd Steury for his advice on accounting for experimental pseudoreplication. I would also like to thank Emily Acer for providing a second pair of eyes for my writing, second pair of hands for my measurements, and overall assistance as a much-needed accountibili-buddy. I am grateful to Nadia Bowles for her friendship and assistance throughout the first part of my degree program, as well as to Hang Li for his help with the setup of this experiment. I would also like to thank Luiza Lazzaro and Rachel Nation, who assisted with the editing of this thesis and provided a welcoming environment for both commiseration and cooperation. I am also grateful to Dr. Scott Enebak for his discerning questions as a member of my committee. Additionally, I would like to thank Michelle Straw and Audrey Grindle for their logistical support. For her substantial assistance in sourcing seedlings, maintaining my experimental plot, editing the Nursery Coop newsletter, and providing advice, I would like to extend my sincere thanks to Nina Payne. I would also like to thank the Southern Forest Nursery Management Cooperative as a whole, as well as the individuals and organizations who provided seedlings for this experiment, including Jeff Fields and Russell Ayres with the Georgia Forestry Commission Nursery, Mike Coyle, Clark Duncan, Brad Clouse, Gretchen Dubs, and DeWayne Hargreaves with the IFCO Moultrie, DeRidder, Jesup, and Pine Hill Nurseries, Thomas Meeks with Meeks Farm and Nursery, Josh Steiger with Rayonier Nursery, Josh Bennicoff with the Virginia Department of Forestry, and Bobby Catrett with the Weyerhaeuser Magnolia Nursery. I would like to extend my sincere thanks to all current and previous members of the Forest and Fire Ecology Lab, my coworkers at Auburn University's College of Forestry, Wildlife, and Environment, and everyone else who was involved with this project. I would also like to thank my funding sources, including the Auburn University College

of Forestry, Wildlife and Environment's Charles D. McCrary Graduate Research, Education, and Training Annual (GREAT) Fellowship, the Alabama Agricultural Experiment Station, and the Hatch program of the National Institute of Food and Agriculture of the U.S. Department of Agriculture. Finally, I would like to thank Ian Goldberg, Monica Haughan, Honey-cat, and my parents for their unending support, kindness, and patience.

Table of Contents

Abstract 2
Acknowledgements 3
List of Tables 6
List of Figures 8
List of Abbreviations and Symbols 10
Introduction 11
Methods 16
Study Design 16
Photosynthesis Measurements 17
Respiration Measurements 19
Growth Measurements 20
Results 23
Temperature Responses of Photosynthetic Parameters: Net Photosynthesis (A_{Net}) 23
Temperature Responses of Photosynthetic Parameters: RuBP Carboxylation Limitations (V_{cmax}) 27
Temperature Responses of Photosynthetic Parameters: RuBP Regeneration Limitations (J_{max}) 31
Temperature Responses of Photosynthetic Parameters: the Ratio of RuBP Regeneration to RuBP Carboxylation (J_{max} to V_{cmax}) 35
Temperature Responses of Dark Respiration 37
Values of $R_{realized}$ at T_{growth} 45
The Ratio of Net Photosynthesis to Dark Respiration 48
Growth 48
Discussion 51
Net Photosynthesis Responds to Variation in Growth Temperature Similarly Across Species 51
Dark Respiration Exhibits Species-Level Adaptation and Acclimation to Growth Temperature 55
Species Show Significantly Different Sizes at Final Harvest 58
Conclusions 59
References 60

List of Tables

Table 1. Provenances, sample sizes at planting and final harvest, and overall mortality rates of planted seedlings are listed by species for loblolly (*Pinus taeda*), longleaf (*Pinus palustris*), shortleaf (*Pinus echinata*), and slash pine (*Pinus elliottii*). ……..……..…… 24

Table 2. Means (± standard error) of net photosynthesis ($A_{Net,25}$) at a measurement temperature of 25 °C, the temperature optimum of A_{Net} ($T_{opt,A}$), the maximum value of A_{Net} (A_{opt}), the value of the coefficient describing the shape of the $T_{opt,A}$ curve (photosynthetic parameter *b*), the ratio of J_{max}:V_{cmax}, and the ratio of $A_{Net,25}$:$R_{dark,25}$ of four southern pine species and related populations. Values marked with * demonstrate a significant positive correlation to the average growth temperature of the thirty days prior to measurement ($T_{growth,30}$), and values marked with ** demonstrate a significant negative correlation to $T_{growth,30}$ ($p < 0.05$). ……..……..... 26

Table 3. Means (± standard error) of the maximum velocity of RuBP carboxylation ($V_{cmax,25}$) at a measurement temperature of 25 °C, the temperature optimum of V_{cmax} ($T_{opt,Vcmax}$), the maximum value of V_{cmax} ($k_{opt,Vcmax}$), and the activation energy of V_{cmax} ($H_{a,Vcmax}$) of four southern pine species and related populations. Values marked with * demonstrate a significant positive correlation to the average growth temperature of the thirty days prior to measurement ($T_{growth,30}$), and values marked with ** demonstrate a significant negative correlation to $T_{growth,30}$ ($p < 0.05$). ……... 30

Table 4. Means (± standard error) of the maximum velocity of RuBP regeneration ($J_{max,25}$) at a measurement temperature of 25 °C, the temperature optimum of J_{max} ($T_{opt,Jmax}$), the maximum value of J_{max} ($k_{opt,Jmax}$), and the activation energy of J_{max} ($H_{a,Jmax}$) of four southern pine species and related populations. Values marked with * demonstrate a significant positive correlation to the average growth temperature of the thirty days prior to measurement ($T_{growth,30}$), and values marked with ** demonstrate a significant negative correlation to $T_{growth,30}$ ($p < 0.05$). ……..... 34

Table 5. Means (± standard error) of the predicted rate of dark respiration ($R_{realized}$) for the average growth temperature on the date of measurement (T_{growth}), the measured rate of dark respiration ($R_{dark,25}$), the rate of respiratory increase per 1 °C increase in measurement temperature ($Q_{10,25}$) at a measurement temperature of 25 °C, and the value of the coefficients describing the slope (log polynomial parameter *b*), curvature (log polynomial parameter *c*), and intercept (log polynomial parameter *a*) of the respiratory temperature response curve of four

southern pine species and related populations. Values marked with * demonstrate a significant positive correlation to the average growth temperature of the thirty days prior to measurement ($T_{growth,30}$), and ** denotes a significant negative correlation with $T_{growth,30}$ ($p < 0.05$). …….. 48
Table 6. Means (± standard error) of root collar diameter, stem length, and dry mass growth metrics at the time of final harvest of four southern pine species and related populations. Superscripts denote statistically significant differences between groups ($p < 0.05$). …….. 51

List of Figures

Figure 1. Population-level variation in net photosynthesis ($A_{Net,25}$) at a measurement temperature of 25 °C compared to the average growth temperature for the thirty days prior to measurement ($T_{growth,30}$). Solid lines represent linear models fit by population (color) and species (black). 25
Figure 2. Population-level variation in net photosynthesis (A_{Net}), compared to the measurement temperature ($T_{measurement}$) across all three measurement campaign months. Solid lines represent quadratic models of net photosynthesis ($T_{opt,A}$) fit by species (black) and population (color). ... 26
Figure 3. Population-level variation in the maximum velocity of RuBP carboxylation ($V_{cmax,25}$) at a measurement temperature of 25 °C compared to the average growth temperature for the thirty days prior to measurement ($T_{growth,30}$). Solid lines represent linear models fit by population (color) and species (black). ……. 29
Figure 4. Population-level variation in the maximum velocity of RuBP carboxylation (V_{cmax}) compared to measurement temperature ($T_{measurement}$) across all three measurement campaign months. Solid lines represent peaked Arrhenius models of V_{cmax} fit by species (black) and population (color). ……..……. 30
Figure 5. Population-level variation in the maximum velocity of RuBP regeneration ($J_{max,25}$) at a measurement temperature of 25 °C compared to the average growth temperature for the thirty days prior to measurement ($T_{growth,30}$). Solid lines represent linear models fit by population (color) and species (black). ……. 33
Figure 6. Population-level variation in the maximum velocity of RuBP regeneration (J_{max}) compared to measurement temperature ($T_{measurement}$) across all three measurement campaign months. Solid lines represent peaked Arrhenius models of J_{max} fit by species (black) and population (color). ……..…….. 34
Figure 7. Population-level variation in the ratio of the maximum velocity of RuBP regeneration (J_{max}) to RuBP carboxylation (V_{cmax}) compared to the average growth temperature for the thirty days prior to measurement ($T_{growth,30}$). Solid lines represent linear models fit by population (color) and species (black). ……..….... 36
Figure 8. Population-level variation in respiration measured in the dark at 25 °C (R_{25}) compared to the average growth temperature during the thirty days prior to measurement ($T_{growth,30}$). Solid lines represent linear models fit by population (color) and species (black). ……... 40

Figure 9. Species-level variation in respiration (R_{dark}) compared to the measurement temperature ($T_{measurement}$). Solid lines represent pseudoexponential models of the temperature response of respiration based on log polynomial models fit by campaign month for each species. …….. 41
Figure 10. Population-level variation in respiration (R_{dark}) compared to the measurement temperature ($T_{measurement}$). Solid lines represent pseudoexponential models of the temperature response of respiration, based on the log polynomial model calculated for each species. …..... 42
Figure 11. Population-level variation in the rate of respiratory increase per 10 °C increase in measurement temperature (Q_{10}) compared to the average growth temperature during the thirty days prior to measurement ($T_{growth,30}$). Solid lines represent linear models fit by species (black) and population (color) ……..…. 43
Figure 12. Population-level variation in the intercepts of the respiratory temperature response curves compared to the average growth temperature during the thirty days prior to measurement ($T_{growth,30}$). Solid lines represent linear models fit by species (black) and population (color). 44
Figure 13. Population-level variation in predicted respiratory rate on the date of measurement ($R_{realized}$) compared to the average growth temperature on the date of measurement (T_{growth}). Solid lines represent linear models fit by species (black) and population (color). ……... 47

List of Abbreviations and Symbols

A_{Net} Rate of net photosynthesis, defined as the leaf-level rate of photosynthesis minus the corresponding rate of respiration

$A_{Net,25}$ Net photosynthesis at a measurement temperature of 25 °C

Log polynomial parameter *a* Coefficient describing the intercept of the respiratory temperature response curve

Log polynomial parameter *b* Coefficient describing the slope of the respiratory temperature response curve

Log polynomial parameter *c* Coefficient describing the curvature of the respiratory temperature response curve

J_{max} Maximum velocity of RuBP (ribulose 1,5-*bis*phosphate) regeneration

$J_{max,25}$ Maximum velocity of RuBP (ribulose 1,5-*bis*phosphate) regeneration at a measurement temperature of 25 °C

Photosynthetic parameter *b* Coefficient describing the shape of the temperature response curve

Q_{10} Rate of respiratory increase per 10 °C increase in measurement temperature

$Q_{10,25}$ Rate of respiratory increase per 10 °C increase in measurement temperature at a measurement temperature of 25 °C

RCD Stem diameter at the root collar

R_{dark} Rate of leaf-level respiration, as measured in the dark

R_{25} Rate of dark respiration at a measurement temperature of 25 °C

T_{growth} Average growth temperature in the field on the date of measurement

$T_{growth,30}$ Average growth temperature in the field during the thirty days prior to measurement

$T_{measurement}$ Manipulated temperature at the time of photosynthesis or respiration measurement

$T_{opt,A}$ Temperature optimum of net photosynthesis, defined as the temperature at which the rate of net photosynthesis is greatest

$T_{opt,Jmax}$ Temperature optimum of RuBP (ribulose 1,5-*bis*phosphate) regeneration

$T_{opt,Vcmax}$ Temperature optimum of RuBP (ribulose 1,5-*bis*phosphate) carboxylation

V_{cmax} Maximum velocity of RuBP (ribulose 1,5-*bis*phosphate) carboxylation

$V_{cmax,25}$ Maximum velocity of RuBP (ribulose 1,5-*bis*phosphate) carboxylation at a measurement temperature of 25 °C

Introduction

By the year 2100, it is projected that the average global surface temperature will increase by 1.4 to 4.4 °C relative to pre-1900 levels (central estimates, SSP1-1.9–SSP5-8.5; Arias *et al.* 2021). While global forests were a net carbon sink of -7.6 ± 49 $GtCO_2e$ yr^{-1} in the period between 2001 and 2019 (Harris *et al.* 2021), forest function can be directly and indirectly affected by temperature (van Mantgem *et al.* 2009; Tiwari *et al.* 2020). Therefore, understanding the existing temperature responses of photosynthesis and respiration in species of interest is critical in order to make accurate predictions of future feedbacks between a changing climate and global forests.

Photosynthesis is the single largest global flux of carbon dioxide, taking up an estimated 123 ± 8 Pg C per year (Beer *et al.* 2010). Mechanistically, photosynthesis involves the conversion of light energy into a chemical form via reactions in the thylakoid membrane (Stirbent *et al.* 2019). This energy is later used in the Calvin-Benson cycle, where the enzyme ribulose bisphosphate carboxylase/oxygenase (Rubisco) catalyzes the fixation of carbon dioxide on RuBP (ribulose 1,5-*bis*phosphate) and RuBP is cyclically regenerated (Stirbent *et al.* 2019). The temperature dependence of net photosynthesis (A_{Net}) can be best understood as the combination of limitations on these component process. Limitations to A_{Net} include the maximum rate of RuBP carboxylation (V_{cmax}; Berry and Björkman 1980; Farquhar *et al.* 1980), the maximum rate of RuBP regeneration (J_{max}; Farquhar *et al.* 1980; Hikosaka *et al.* 2005), the efficiency of triose phosphate utilization (*TPU*; Hikosaka *et al.* 2006; Yang *et al.* 2016), the intercellular concentration of CO_2 (C_i; Berry and Björkman 1980; Flexas *et al.* 2012; Wang *et al.* 2020), and the rate of respiration (R; Atkin and Tjoelker 2003).

V_{cmax} reflects limitations on the activity of Rubisco, and therefore the overall rate of photosynthesis, with changes in temperature (Berry and Björkman 1980). Rubisco can alternatively catalyze a carboxylation reaction as part of the Calvin-Benson cycle or an oxygenation reaction as part of an opposing photorespiratory pathway (Andersson and Backlund 2008). At temperatures below the photosynthetic temperature optimum ($T_{opt,A}$), the rate of carbon assimilation typically increases with temperature due to the kinetics of the Rubisco-catalyzed carboxylation reaction (Berry and Björkman 1980; Hermida-Carrera *et al.* 2016). However, above the $T_{opt,A}$, the rate of carboxylation increases slower than the rate of oxygenation due to a decreased affinity of Rubisco for CO_2 and decreased concentration ratio of CO_2 to O_2 in solution (Sage *et al.* 2008; Hermida-Carrera *et al.* 2016). Although the thermal stability varies by species,

Rubisco has been found to be heat stable at temperatures in excess of 49.5 °C (Björkman *et al*. 1978), while substantial Rubisco activase denaturation has been observed at temperatures as low as 37 °C (Salvucci *et al*. 2001). The denaturation of Rubisco activase would theoretically cause a reduction in the activation level of Rubisco within the chloroplast, resulting in a slowing of the Calvin-Benson cycle (Sage *et al.* 2008). Therefore, V_{cmax} limitations can describe a combination of enzymatic kinetics, CO_2 concentration, and activation state on the activity of Rubisco *in vivo*.

J_{max} limitations refer to processes related to the regeneration of RuBP at the end of the Calvin-Benson cycle (Farquhar *et al*. 1980). As RuBP is the key acceptor of CO_2 in the Calvin-Benson cycle (Stirbent *et al.* 2019), RuBP deficits can result in major limitations to the overall rate of photosynthesis. While the limiting step of RuBP regeneration may differ between species or temperatures (Hikosaka *et al.* 2006), J_{max} limitations are typically linked to declines in thylakoid membrane electron transport activity (Berry and Björkman 1980). At high temperatures, structural changes in the thylakoid membrane can result in increased ion leakage and decreased proton motive force (Sharkey and Zhang 2010), while low temperatures can result in increased membrane saturation and reduced electron carrier diffusion (Niinemets *et al.* 1999). In a similar vein, low electron transport chain capacity may contribute to a *TPU* limitation, which occurs when triose phosphates from the Calvin cycle cannot be converted into other sugars quickly enough to keep pace with the rate of photosynthesis (Yang *et al.* 2016). Although *TPU* limitations are typically only relevant at very low temperatures (Yang *et al.* 2016), the electron transport chain limitations described by J_{max} remain a major limitation to A_{Net} under physiologically relevant temperature conditions.

As CO_2 acts as one of two potential substrates for Rubisco, the concentration of CO_2 available inside the leaf is another major determinant of the overall rate of photosynthesis. C_i is limited by stomatal conductance (g_s), which refers to the rate of diffusion of CO_2 from the atmosphere to the sub-stomatal cavity (Wang *et al*. 2020), and mesophyll conductance (g_m), which refers to the rate of diffusion of CO_2 through intercellular spaces, cell walls, and the intercellular liquid pathway within the mesophyll (Flexas *et al.* 2008). While stomatal conductance has been observed to increase with increasing temperature (Urban *et al.* 2017), assessments of the influence of temperature on g_m remain scarce due to the challenges inherent in g_m measurement (Flexas *et al*. 2008).

Finally, A_{Net} can be influenced by the temperature responses of *R*. Respiration and photosynthesis share a complex regulatory relationship involving the use of mitochondria-generated ATP for photosynthetic processes, mitochondrial dissipation of excess photosynthetic reducing agents, and joint involvement in the photorespiratory pathway (Millar *et al.* 2011). Therefore, a full understanding of carbon flux dynamics within an individual plant requires an appreciation of photosynthetic and respiratory processes both in isolation and in the context of one another.

Due to the numerous temperature-dependent reactions involved, the temperature responses of *R* are best understood as a composite of multiple components. At low temperatures, *R* can be limited by the kinetics of enzymes involved in glycolysis or the citric acid cycle (V_{max}) or by a reduction in electron transport chain function due to an increase in membrane rigidity (Atkin and Tjoelker 2003). At moderate temperatures, the rate of respiration can be limited by substrate and adenylate availability (Atkin and Tjoelker 2003). Finally, at extremely high temperatures, low membrane thermal stability can result in the loss of concentration gradients, further reducing substrate availability and resulting in higher respiratory requirements in order to maintain plant functionality (Atkin and Tjoelker 2003; Mohammed and Tarpley 2009). The change in overall limiting factor from enzymatic capacity to substrate or adenylate availability results in a greater increase in respiratory rate per degree Celsius for cold temperatures than warm temperatures (Atkin and Tjoelker 2003). The temperature dependence of *R* at a given temperature can be quantified through the value of Q_{10}, or the proportional increase in *R* per 10 °C (Atkin and Tjoelker 2003; Aspinwall *et al.* 2017a).

Photosynthetic and respiratory responses to temperature are not static, and changes can occur at a variety of ecological and temporal scales. Short-term, reversible changes in an individual's phenotype that provide a fitness advantage in the context of an immediate environmental stressor are referred to as acclimation (Berry and Björkman 1980; Aspinwall *et al.* 2017b), while multi-generational, genetic changes that improve a species' or population's fitness in the context of a long-term selective pressure are referred to as adaptation (Aspinwall *et al.* 2017b; Collier *et al.* 2019). In practice, there can be significant overlap in physiological acclimation and adaptation, as genetic factors determine an individual's acclimation potential, or the extent to which an individual can alter its phenotype in response to environmental stressors (Berry and Björkman 1980). Both adaptive and acclimatory changes must be considered in order

to fully understand the potential effects of increasing global surface temperatures on the physiological processes of carbon uptake and release.

Photosynthetic adaptation to temperature can occur through a number of mechanisms, including the specialization of photosynthetic proteins (Fernández-Marín *et al*. 2020) and heritable changes to membrane composition (Guschina and Harwood 2006). While an analysis of global photosynthesis datasets found no predictable relationship between $T_{opt,A}$ and climate of origin, global variation in $T_{opt,A}$ was strongly driven by variation in growth temperature, leading the authors to hypothesize that photosynthetic temperature acclimation may swamp out the less influential effects of adaptation (Kumarathunge *et al*. 2018). Photosynthetic acclimation can occur through reversible changes to the structure and concentration (Yamori *et al.* 2005) or activation state of photosynthetic proteins (Sage *et al.* 2008), short-term alterations to thylakoid membrane structure (Yamori *et al.* 2014), or changes of stomatal and mesophyll conductance (Yamori *et al.* 2005; Wang *et al.* 2020).

The genetic variation and temperature acclimation of R is often correlated with that of A_{Net} (Dusenge *et al.* 2019). Unlike photosynthesis, however, prior metanalyses of respiratory adaptation to temperature have found differences in basal respiratory rate between plant functional types and biomes (Heskel *et al.* 2016). While the mechanisms of respiratory adaptation in plants remain unclear, respiratory adaptation to temperature likely involves changes to the mitochondrial genome (Das 2006). The temperature acclimation of R may occur through changes in a plant's temperature sensitivity, measured through a change in Q_{10} (Type I), or through a shift in the overall intercept of the temperature-response curve (Type II; Atkin and Tjoelker 2003). While Type I acclimation can involve short-term changes in soluble sugar availability (Atkin *et al.* 2000), Type II acclimation is typically driven by an increase in enzymatic capacity (Wei *et al*. 2016). Additionally, while both Type I and Type II respiratory acclimation can affect the observed rate of respiration at moderate to high temperatures, only Type II acclimation can substantially alter the rates of respiration observed at low temperatures (Atkin and Tjoelker 2003). Partial Type II acclimation can be commonly found across plant types and biomes (Slot and Kitajima 2015; Zhu *et al.* 2021), although there is a wide range of variation in the responses of individual species and populations (Bolstad *et al.* 2003; Tjoelker *et al*. 2009; Silim *et al.* 2010; Aspinwall *et al.* 2017b). It should be noted that most studies assessing the temperature acclimation of R focus on leaf-level mitochondrial respiration as

measured in the dark (R_{dark}; Way and Yamori 2013), as the presence of light typically suppresses the rate of respiration during the day (R_{light}; Way *et al.* 2015).

The adaptation and acclimation of photosynthesis and respiration to temperature can substantially change how an increasing global surface temperature will affect forests around the world, with potential implications for carbon feedback modeling (Rogers *et al.* 2017), future ecosystem structures (Ghannoum and Way 2011), and the forestry industry (Kirilenko and Sedjo 2017). In the southeastern United States, loblolly pine (*Pinus taeda*) remains the predominant timber species (Schultz 1999), and the southeastern forest products industry employs over 700,000 people and provides $82 billion in value added to the region (Jolley *et al.* 2020). Therefore, understanding the potential direct and indirect effects of increasing global temperature on southern pine productivity can have substantial social and economic impacts throughout the region. Temperature-induced alterations to the productivity of southern pines may also have substantial ecological impacts across the southeastern United States. Longleaf pine (*Pinus palustris*) provides habitat for dozens of threatened or endangered animal species and over 180 rare plant species (Van Lear *et al.* 2005), while both longleaf and shortleaf pine (*Pinus echinata*) provide habitat for the federally listed red-cockaded woodpecker (*Picoides borealis*; Bukenhofer *et al.* 1994; Van Lear *et al.* 2005). Similarly, slash pine (*Pinus elliottii*) serves as a keystone species for the highly endangered and rapidly disappearing pine rockland habitat of southern Florida (Williams *et al.* 2007).

Despite the multitude of ecosystem services provided by southern pines, relatively little research has been conducted into the temperature responses of photosynthesis and respiration in key southern pine species. While Teskey and Will (1999) observed evidence of respiratory adaptation and photosynthetic and respiratory acclimation to temperature in loblolly pine, Samuelson *et al.* (2012) found no evidence of differences in photosynthetic rate among species or photosynthetic acclimation to temperature in loblolly, longleaf, or slash pine. Similarly, while Wells and Wakeley (1970) found evidence of different growth rates due to provenance in shortleaf pine, the authors are not aware of any studies explicitly testing the temperature acclimation of photosynthesis or respiration in shortleaf pine. Therefore, the responses of photosynthesis and respiration to temperature currently remain unclear for loblolly, longleaf, slash, and shortleaf pine.

To address this knowledge gap, this study measured and compared the temperature adaptation and acclimation potential of leaf-level photosynthesis and respiration across loblolly, longleaf, slash, and shortleaf pine. Based on the likely evolutionary pressures faced by these species, we hypothesized that species and populations from warmer and lower latitude home climates would demonstrate higher $T_{opt,A}$ and lower rates of realized respiration than species and populations from more temperate home climates. Additionally, we hypothesized that species with wider home ranges and populations from more seasonal home climates would demonstrate a greater extent of photosynthetic and respiratory temperature acclimation.

Methods

Study Design

Seedlings were sampled from one year old, nursery-grown seedlings of loblolly pine (*Pinus taeda*), longleaf pine (*Pinus palustris*), shortleaf pine (*Pinus echinata*), and slash pine (*Pinus elliottii*). Seedlings were sourced from three to four geographically distinct provenances throughout each species' range in collaboration with the Southern Forestry Management Cooperative. All loblolly and slash pine seedlings were bareroot, and all longleaf and shortleaf pine seedlings were containerized. Despite the maintenance of non-limiting nutrient and water availability conditions, the shortleaf pine seedlings suffered substantial (70.69%) rates of mortality. Therefore, a second set of shortleaf pine seedlings was planted in mid-March. The overall mortality rate across all species and populations was 35.22% (Table 1).

A common garden experiment was established at the trophotron research site at Auburn University in Auburn, Alabama, USA (32.59° N, 85.49° W). Seedlings were arranged using a split-plot design, with species at the whole-plot level and population at the subplot level. Species position was randomly determined within each of six blocks, then population positions were randomly determined within each species plot. Finally, individual seedlings were randomly assigned to each population position. Slight modifications in seedling distribution across all ssix blocks were made in response to seedling mortality prior to the first measurement campaign.

All seedlings were planted into identical 22.86 by 39.37 cm pots (Stuewe and Sons, Inc. 2023) in a top soil growing medium (Evergreen 2022). Seedlings were planted between October 2021 and March 2022 within 48 hours of arrival from the nursery of origin. Throughout the experiment's duration, seedlings were watered every one to three days according to weather and

soil moisture conditions. Soil moisture was measured periodically throughout the study duration using a HydroSense II soil moisture probe to a depth of 20 cm (Campbell Scientific, Inc. 2020), and soil moisture content for all seedlings was maintained between an average of 11.48% (± 9.74; 95% CI) and 24.36% (± 11.82; 95% CI). All seedlings were fertilized with 25 mL of a 10N:10P_2O_5:10K_2O formula every two to four weeks to avoid nutrient limitations (Winston Weaver Co., Inc. 2022). After an outbreak of brown spot needle blight (*Scirrhia acicula*) in October 2022, all longleaf seedlings were treated with 5 oz/ac equivalent of Proline fungicide (Bayer CropScience LP 2019).

A HOBO U30 weather station and associated sensors were used to provide continuous readings of ambient temperature, relative humidity, solar radiation, and wind speed and direction at ten minute intervals from February 2021 through the study's conclusion (HOBO Data Loggers 2020). Growth temperatures were calculated from the average air temperature recorded for the thirty days immediately prior to the date of measurement ($T_{growth,30}$) or on the date of measurement (T_{growth}). A 16.80 °C range of seasonal temperature variation in $T_{growth,30}$ and a 26.05 °C range of seasonal temperature variation in T_{growth} were captured in this study. Due to the nature of actual seasonal variation in the field, photoperiod covaried with growth temperature at the study site.

Photosynthesis Measurements

Photosynthesis measurement campaigns were conducted at three timepoints during the study's duration: June 7-23, 2022, October 2-24, 2022, and January 7-24, 2023. Prior to each measurement campaign, one individual from each population within each block was randomly selected for measurement (n=78). Each day, a random subset of selected seedlings was taken to an indoor, temperature- and light-controlled growth chamber and allowed to adjust to the temperature in the chamber for twenty minutes. Using LI-6800 portable photosynthesis systems (LI-COR Biosciences 2021), a net photosynthesis (A_{net}) measurement was made at an ambient (420 μmol mol^{-1}) CO_2 concentration for three mature fascicles (approximately nine needles) per individual. Following the spot measurement, photosynthetic CO_2 response (A/C_i) curves were measured at 11 CO_2 concentrations ranging from 0 μmol mol^{-1} to 1800 μmol mol^{-1}. The process was repeated at 5°C increments ranging from 15°C to 40°C for all sampled individuals. During the course of this experiment, photosynthetically active radiation exposure was held constant at 1800 μmol m^{-2} s^{-1}. Water vapor was introduced or removed from the measurement chamber as

necessary to approximate a target relative humidity of 50%. Needle widths were recorded at the time of measurement in October and January and at the time of collection in June, allowing photosynthesis to be expressed on a leaf area basis. All measurement protocols used were based on Aspinwall *et al.* (2017b).

Datasheets for measurements of photosynthesis were downloaded from the LI-6800 systems, and measured values of needle width were manually entered. Using R programming language version 4.2.1 (R Core Team 2022), values of A and C_i below 0 were removed from analysis. Next, A/C_i curves were examined graphically, and influential outliers were removed. A/C_i curves were fitted according to the Farquhar *et al.* (1980) biochemical model using the *plantecophys* package (Duursma 2015). Curves were preferentially fit using the default approach with no temperature correction. Curves that could not be fit using the default method were fit using a bilinear approach. Model fit was assessed through a linear regression of observed vs. fitted points. Kept curves were required to have a trendline slope within 0.25 of 1 and an R^2 above 0.5. Any A/C_i curve with fewer than six valid points was excluded from further analysis. After the quality control process was complete, a total of 1210 curves from 224 individuals were used in T_{opt} analysis.

Peaked Arrhenius models were fit to the temperature responses of V_{cmax} and J_{max} using A/C_i curve data, as described in Medlyn *et al*. (2002). T_{opt}, K_{opt}, and H_a were determined iteratively, while H_d was fixed at 200 kJ mol^{-1} to avoid over-parameterization. A peaked Arrhenius model approach was selected due to its grounding in biochemical theory regarding limitations to the activity of Rubisco (Scafaro *et al.* 2023) and empirical observation (Medlyn *et al*. 2002; Kattge and Knorr 2007). The T_{opt} of A was determined using A_{net} data via a quadratic model according to Aspinwall *et al.* (2017b) and Battaglia *et al.* (1996). All T_{opt} models required at least four datapoints to successfully converge. All models that failed to successfully converge or that generated a minimum instead of a maximum value were removed from analysis. Additionally, all A models that generated a $T_{opt,A}$ above 50 °C or below 5 °C were removed from analysis, as the calculated temperature optima were substantially outside of the range of experimentally measured temperatures. A total of 116 individuals were used for fitting models of $T_{opt,Vcmax}$ and $T_{opt,Jmax}$, and 176 individuals were used for fitting models of $T_{opt,A}$. All T_{opt} models were fit using a nonlinear least-squares regression approach using the *minpack.lm* package (Elzhov *et al.* 2022).

The mean air temperature at the common garden site during the thirty days prior to each measurement ($T_{growth,30}$) was included as a predictor variable in all models. To avoid the potential for substantial pseudoreplication, date was included as a random effect in all species-level models of photosynthesis. As fewer than 15% of all population-level photosynthesis measurements were pseudoreplicated, no random effects were incorporated for population-level photosynthetic analyses. As location within the plot was found to have no significant effect, all locations were grouped for analysis. All mixed effect ANCOVAs were conducted using the *nlme* package (Pinheiro *et al.* 2023). All fixed effect ANCOVAs and Tukey HSD post-hoc tests were conducted using commands available in base R, with the addition of the Type III ANOVA analysis available through the *car* package (Fox and Weisberg 2019) and the Tukey HSD post-hoc test available through the *emmeans* package (Lenth *et al.* 2023) for models containing random effects. Standard errors were calculated using the package *plotrix* (Lemon *et al.* 2009).

Respiration Measurements

Respiration measurement campaigns were conducted at five timepoints during the study's duration: June 24-26, 2022, August 21-23, 2022, October 28-November 5, 2022, December 9-11, 2022, and January 25-27, 2023. Prior to each measurement campaign, one individual from each population within each block was randomly selected for measurement (n=78), then randomly assigned to one of three measurement days. Before dawn (between 04:00 and 06:00), three mature fascicles were detached from each of the selected seedlings and stored in darkness with a damp paper towel. LI-6800 systems were used to measure CO_2 efflux, an indicator of cellular respiration (R_{dark}), in complete darkness following the same measurement temperature regime as photosynthesis. Needles were then dried and weighed so that respiration could be expressed on a dry mass basis.

Measured values of needle dry weight were manually entered into LI-6800 datasheets of respiration measurements, and any values of R above 0 were removed. Next, a log polynomial model was used to describe the temperature response of R_{mass} for each individual according to the methodology of O'Sullivan *et al.* (2013). The log polynomial coefficients for each individual were then used to calculate a value of Q_{10} for each available measurement temperature. Upon comparison to the fit of a purely exponential Q_{10} model, which assumes a constant value of Q_{10} across measurement temperatures (Tjoelker *et al.* 2009), the log polynomial-derived Q_{10} model was found to provide a substantially better fit to the data. Therefore, the log polynomial-derived

values of Q_{10} were used for all future analysis, including to predict the rate of respiration expected for the average growth temperature experienced on the date of measurement. T_{leaf} was assumed to be equal to T_{air} for all measurements. The log polynomial models were fit using a linear model-based approach, while all Q_{10} values were determined iteratively using a nonlinear least-squares regression approach. A total of 379 individuals were used for fitting models of Q_{10}.

The mean air temperature at the common garden site during the thirty days prior to each measurement ($T_{growth,30}$) was included as a predictor variable in all models. To avoid the potential for substantial pseudoreplication, date was included as a random effect in all models of respiration. As location within the plot was found to have no significant effect, all locations were grouped for analysis. All mixed effect ANCOVAs were conducted using the *nlme* package (Pinheiro *et al.* 2023), with the addition of the Type III ANOVA analysis available through the *car* package (Fox and Weisberg 2019), the Tukey HSD post-hoc test available through the *emmeans* package (Lenth *et al.* 2023), and the standard error calculation available through the *plotrix* package (Lemon *et al*. 2009).

Growth Measurements

At the time of planting, one to three seedlings for each population (n=88) were destructively sampled to allow for estimations of initial shoot length, root collar diameter (*RCD*), dry root mass, dry shoot mass, and dry leaf mass. Measurements of shoot length and diameter at 5 cm above the root collar were conducted on all living seedlings in December 2021, August 2022, December 2022, and February 2023. Measurements of stem diameter were recorded at 5 cm above the root collar to avoid disturbing the growth of the living seedlings. A subset of all living seedlings (n=138) was destructively sampled at the study's conclusion in February 2023, and measurements were obtained for final shoot length, *RCD*, diameter at 5 cm above the root collar, dry root mass, dry shoot mass, and dry leaf mass. Some root systems were collected in an incomplete form, as part of the root system had grown outside of the pot and become irretrievable at the time of final harvest.

Best fit models for the prediction of *RCD* and total dry weight were selected using a bidirectional stepwise selection procedure via the *MASS* package (Ripley *et al.* 2023). Predictive ability of the best fit models was assessed using a 10-fold cross-validation procedure via the *caret* package (Kuhn *et al.* 2023). The best fit models were used to generate estimated values of initial, mid-study, and final *RCD* and total dry weight for all individuals with measured stem

lengths and diameters at 5 cm above the root collar. For all non-destructive measurements, *RCD* was estimated from the diameters at 5 cm above the root collar using the relationship obtained from final harvest data. As the diameters at 5 cm above the root collar could not be measured for grass-stage longleaf pine seedlings at the time of initial planting, initial diameters at 5 cm above the root collar were modeled for longleaf pine using data obtained at the time of final harvest. Differences in final *RCD*, stem length, and dry weight between species and populations were assessed using ANOVAs and Tukey HSD post-hoc tests.

Table 1. Provenances, sample sizes at planting and final harvest, and overall mortality rates of planted seedlings are listed by species for loblolly (*Pinus taeda*), longleaf (*Pinus palustris*), shortleaf (*Pinus echinata*), and slash pine (*Pinus elliottii*).

Species	Population	Initial Sample Size	Final Sample Size	Mortality Rate
Loblolly		125	105	16.00%
	Tuscaloosa County, AL	32	31	3.13%
	Drew County, AR	32	26	18.75%
	Marion County, FL	31	18	41.94%
	Twiggs County, GA	30	30	0.00%
Longleaf		92	68	26.09%
	Unknown, AL	32	24	25.00%
	Escambia County, FL	27	24	11.11%
	Unknown, NC	33	20	39.39%
Shortleaf		116 (66 Dec, 50 March)	34	70.69%
	Unknown, AR	39 (22 Dec, 17 March)	17	56.41%
	Unknown, MS	39 (22 Dec, 17 March)	7	82.05%
	Unknown, TX	38 (22 Dec, 16 March)	10	73.68%
Slash		90	67	25.56%
	Flagler County, FL	30	18	40.00%
	Tattnall County, GA	30	27	10.00%
	Sabine Parish, LA	30	22	26.67%
All	All	423	274	35.22%

Results

Temperature Responses of Photosynthetic Parameters: Net Photosynthesis (A_{Net})

For each 1 °C increase in $T_{growth,30}$, the mean value of $A_{Net,25}$ across all species and populations increased by 0.41 μmol m^{-2} s^{-1} (± 0.078 SE; $p < 0.0001$). No significant differences in the value of $A_{Net,25}$ were found between species or populations (Table 2; $p > 0.05$), and the differences in the response of $A_{Net,25}$ to $T_{growth,30}$ between species and populations were not statistically significant (Figure 1; $p > 0.05$). Additionally, no significant differences in the average temperature optimum of photosynthesis ($T_{opt,A}$) or in the response of $T_{opt,A}$ to $T_{growth,30}$ were observed at the species or population level (Table 2; $p > 0.05$). When averaged across all populations and species, each 1 °C increase in $T_{growth,30}$ resulted in a decrease in the value of $T_{opt,A}$ of 0.29 °C (± 0.062 SE; Figure 2; $p < 0.0001$). Although significant differences in the maximum value of net photosynthesis (A_{opt}) between species and in the response of A_{opt} to $T_{growth,30}$ were observed at the species level ($p < 0.05$), post-hoc analysis failed to uncover any significant pairwise comparisons (Table 2; $p > 0.05$). Similarly, no significant differences in the value of A_{opt} or in the response of A_{opt} to $T_{growth,30}$ were observed between populations ($p > 0.05$). For each 1 °C increase in $T_{growth,30}$, the mean A_{opt} of all species and populations increased by 0.42 μmol m^{-2} s^{-1} (± 0.070 SE; Figure 2; $p > 0.0001$). No significant differences in the average value of the coefficient describing the shape of the $T_{opt,A}$ curve (photosynthetic parameter *b*) were found between species or populations, and no significant differences were observed in the response of parameter *b* to $T_{growth,30}$ at the species or population level (Table 2; $p > 0.05$). When all species and populations were grouped for analysis, the mean value of photosynthetic parameter *b* increased by units (± SE) for each 1 °C increase in $T_{growth,30}$ (Figure 2; p). In summary, the temperature response of A_{Net} was relatively similar across species and populations. The value of $A_{Net,25}$, A_{opt}, and photosynthetic parameter *b* increased significantly with increasing $T_{growth,30}$, although some photosynthetic parameters, including $T_{opt,A}$, demonstrated a significant decrease with increasing $T_{growth,30}$. Despite the surprising temperature response of $T_{opt,A}$, species and populations exhibited significant evidence of photosynthetic acclimation to temperature, with little variation in the overall extent of acclimation between groups.

Table 2. Means (± standard error) of net photosynthesis ($A_{Net,25}$) at a measurement temperature of 25 °C, the temperature optimum of A_{Net} ($T_{opt,A}$), the maximum value of A_{Net} (A_{opt}), the value of the coefficient describing the shape of the $T_{opt,A}$ curve (photosynthetic parameter *b*), the ratio of J_{max}:V_{cmax}, and the ratio of $A_{Net,25}$:$R_{dark,25}$ of four southern pine species and related populations. Values marked with * demonstrate a significant positive correlation to the average growth temperature of the thirty days prior to measurement ($T_{growth,30}$), and values marked with ** demonstrate a significant negative correlation to $T_{growth,30}$ ($p < 0.05$).

		A_{Net}				Ratios	
Species	Population	$A_{Net,25}$ (μmol m^{-2} s^{-1})	$T_{opt,A}$ (° C)	A_{opt} (μmol m^{-2} s^{-1})	Parameter *b*	$J_{max,25}$:$V_{cmax,25}$	$A_{Net,25}$:$R_{Net,25}$
All		8.97 ± 0.41*	25.24 ± 0.44**	9.16 ± 0.40*	0.025 ± 0.0013*	1.42 ± 0.029**	1.06 ± 0.055*
Longleaf		8.89 ± 0.83*	26.27 ± 0.81	10.35 ± 0.70	0.033 ± 0.00031	1.57 ± 0.057**	1.10 ± 0.10*
	Alabama	10.31 ± 1.36	22.69 ± 1.49	11.06 ± 1.26	0.030 ± 0.0045	1.64 ± 0.087**	1.29 ± 0.17
	Florida	8.80 ± 1.54*	26.19 ± 0.77	10.38 ± 1.26	0.035 ± 0.0040	1.49 ± 0.068	1.12 ± 0.20*
	N. Carolina	7.25 ± 1.37	30.21 ± 1.35	9.54 ± 1.14	0.035 ± 0.0080*	1.57 ± 0.13**	0.86 ± 0.16
Loblolly		8.03 ± 0.74*	24.89 ± 0.83	7.87 ± 0.67*	0.018 ± 0.0016	1.42 ± 0.045	1.04 ± 0.11*
	Alabama	8.67 ± 2.02*	25.49 ± 1.89	9.43 ± 1.64	0.019 ± 0.0036	1.38 ± 0.10	1.18 ± 0.27*
	Arkansas	6.99 ± 1.14	26.21 ± 1.47	6.70 ± 0.83	0.017 ± 0.0030	1.44 ± 0.080	0.84 ± 0.20*
	Florida	8.45 ± 1.50*	26.04 ± 0.87	8.36 ± 1.48*	0.022 ± 0.0029	1.44 ± 0.087	1.13 ± 0.22*
	Georgia	7.99 ± 1.11	21.76 ± 1.96	6.89 ± 1.23*	0.016 ± 0.0029	1.43 ± 0.11**	0.94 ± 0.19
Shortleaf		9.48 ± 0.78*	23.69 ± 0.92**	9.53 ± 0.78*	0.026 ± 0.0032	1.29 ± 0.072**	0.96 ± 0.10*
	Arkansas	9.99 ± 1.44*	23.28 ± 1.32	9.37 ± 1.35	0.029 ± 0.0055	1.47 ± 0.11	1.07 ± 0.21*
	Mississippi	9.86 ± 1.48	23.50 ± 1.58	10.46 ± 1.44	0.029 ± 0.0070	1.00 ± 0.13	0.97 ± 0.17
	Texas	8.62 ± 1.19	24.37 ± 2.01**	8.71 ± 1.32	0.017 ± 0.0024	1.28 ± 0.072	0.86 ± 0.15*
Slash		9.83 ± 0.94*	25.97 ± 0.96**	9.00 ± 1.00*	0.022 ± 0.0019	1.35 ± 0.040	1.19 ± 0.12
	Florida	8.95 ± 1.00	27.42 ± 1.47	8.08 ± 1.39	0.020 ± 0.0028	1.49 ± 0.081	1.08 ± 0.18
	Georgia	8.79 ± 1.72	27.26 ± 1.30**	8.36 ± 1.62**	0.021 ± 0.0030	1.33 ± 0.036	1.03 ± 0.16
	Louisiana	11.33 ± 1.83	23.50 ± 1.96**	10.37 ± 2.05**	0.024 ± 0.0037	1.21 ± 0.055	1.38 ± 0.24

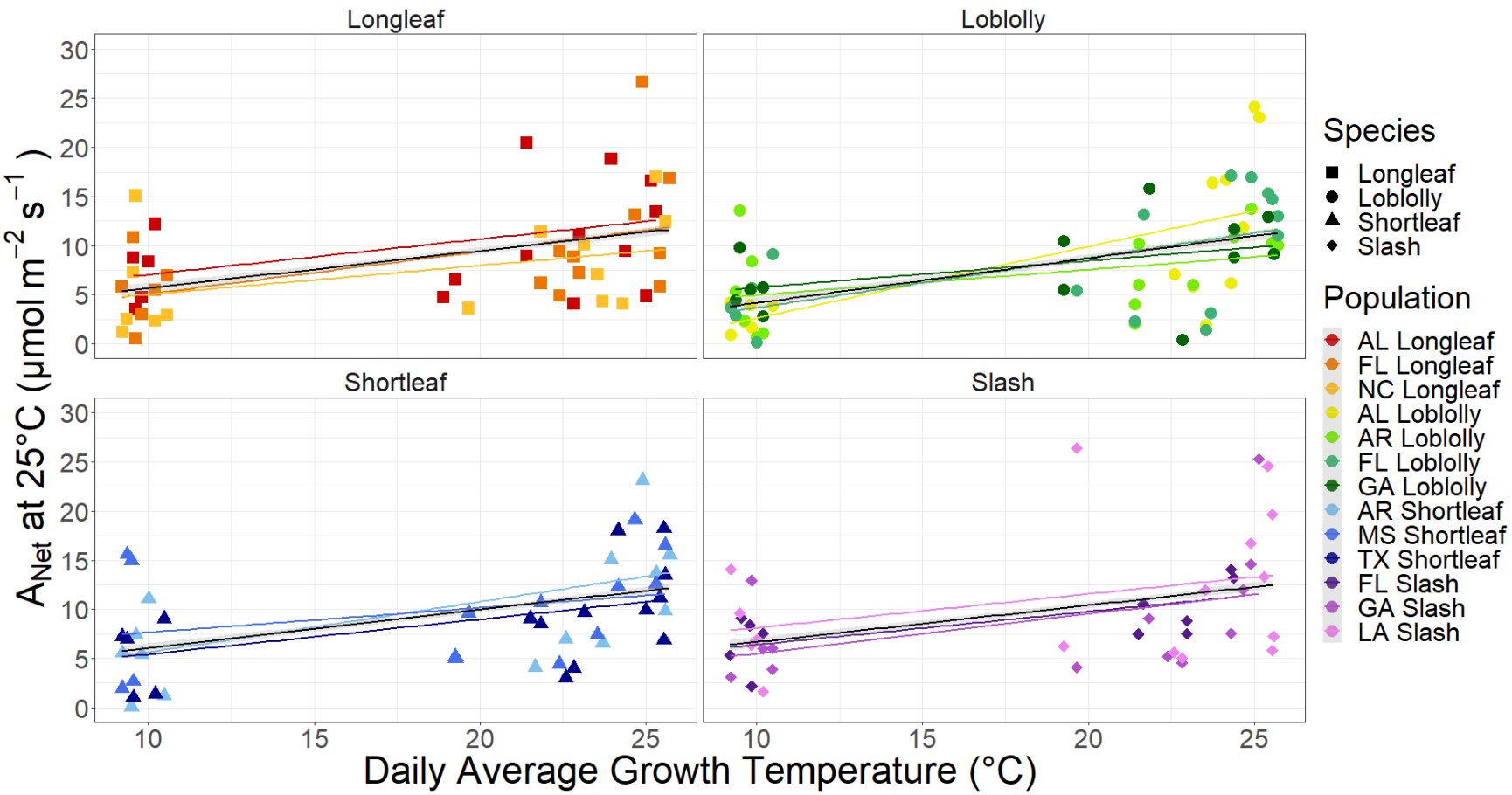

Figure 1. Population-level variation in net photosynthesis ($A_{Net,25}$) at a measurement temperature of 25 °C compared to the average growth temperature for the 30 days prior to measurement ($T_{growth,30}$) for four southern pine species and related populations. Solid lines represent linear models fit by population (color) and species (black).

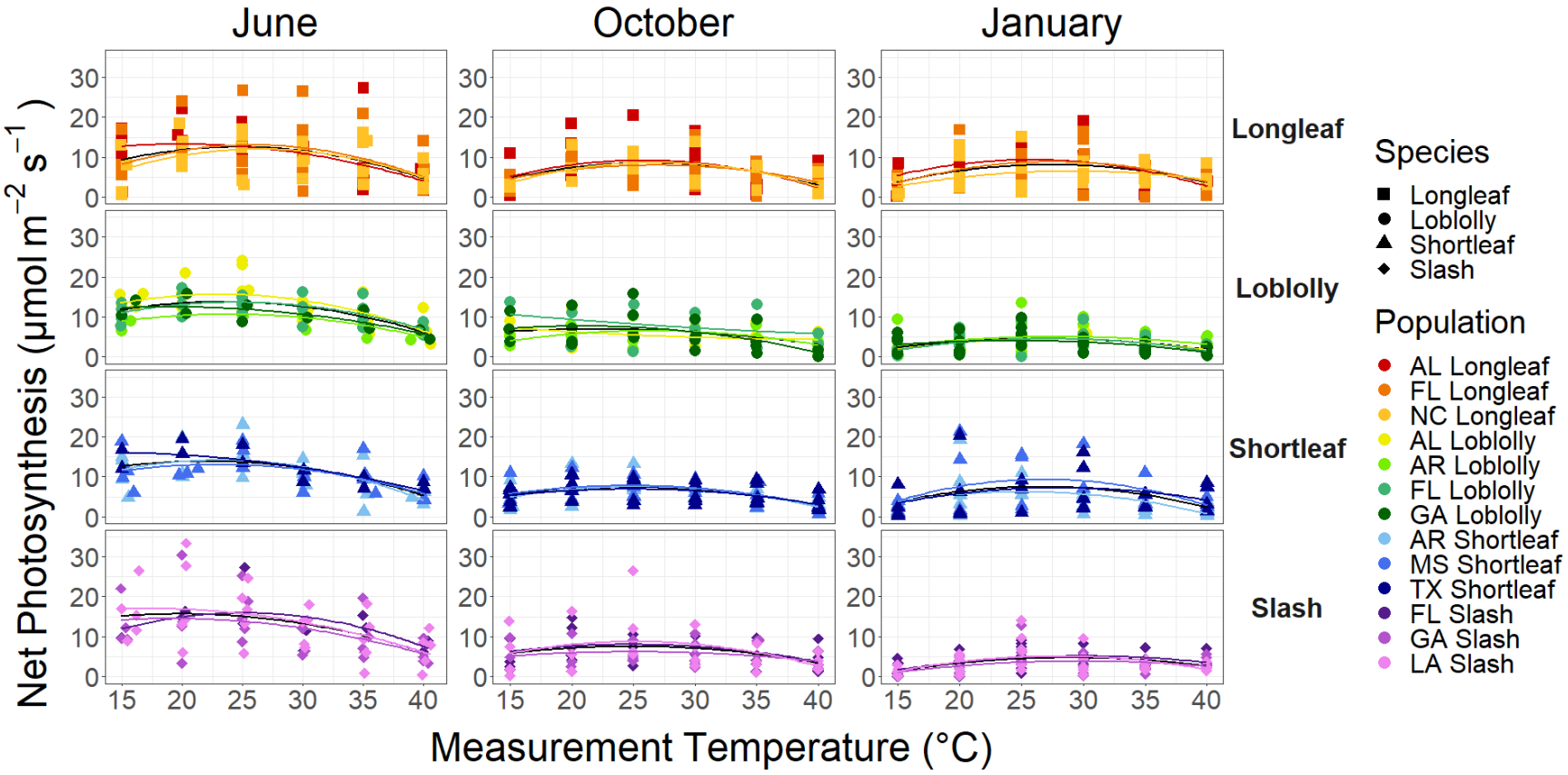

Figure 2. Population-level variation in net photosynthesis (A_{Net}), compared to the measurement temperature ($T_{measurement}$) across three measurement campaign months for four southern pine species and related populations. Solid lines represent quadratic models of net photosynthesis ($T_{opt,A}$) fit by species (black) and population (color).

Temperature Responses of Photosynthetic Parameters: RuBP Carboxylation Limitations (V_{cmax})

No significant differences in the in the maximum velocity of RuBP carboxylation at a measurement temperature of 25 °C ($V_{cmax,25}$) or in the response of $V_{cmax,25}$ to $T_{growth,30}$ were exhibited between species or populations (Table 3; $p > 0.05$). For each 1 °C increase in $T_{growth,30}$, the value of $V_{cmax,25}$ across all species and populations increased by 1.19 μmol m^{-2} s^{-1} (± 0.44 SE; Figure 3; $p = 0.0068$). Similarly, no significant differences in the average temperature optimum of V_{cmax} ($T_{opt,Vcmax}$) were observed between species or populations, and no significant differences in the response of $T_{opt,Vcmax}$ to $T_{growth,30}$ were observed between species or populations (Table 3; $p > 0.05$). For each 1 °C increase in $T_{growth,30}$, the average value of $T_{opt,Vcmax}$ for all species and populations increased by 0.14 °C (± 0.058 SE; Figure 4; $p = 0.021$). No significant differences in the maximum value of V_{cmax} ($k_{opt,Vcmax}$) were found between species or populations (Table 3; $p > 0.05$), and no significant differences were found in the response of $k_{opt,Vcmax}$ to $T_{growth,30}$ between species or populations ($p > 0.05$). The mean value of $k_{opt,Vcmax}$ for all species and populations increased by 2.36 μmol m^{-2} s^{-1} (± 0.81 SE) for each 1 °C increase in $T_{growth,30}$ (Figure 4; $p = 0.0037$). Finally, no significant differences in the activation energy of V_{cmax} ($H_{a,Vcmax}$) were found between species or populations, and no significant differences were observed in the response of $H_{a,Vcmax}$ to $T_{growth,30}$ at the species or population level ($p > 0.05$). When all species and populations were grouped for analysis, the mean value of $H_{a,Vcmax}$ decreased by 1.24 kJ mol^{-1} (± 0.60 SE) for each 1 °C increase in $T_{growth,30}$ (Figure 4; $p = 0.039$). Across metrics of V_{cmax}, all species and populations demonstrated a similar acclimatory response to temperature, with the mean values of $V_{cmax,25}$, $T_{opt,Vcmax}$, and $k_{opt,Vcmax}$ increasing with increasing $T_{growth,30}$ and the mean value of $H_{a,Vcmax}$ decreasing with increasing $T_{growth,30}$.

Table 3. Means (± standard error) of the maximum velocity of RuBP carboxylation ($V_{cmax,25}$) at a measurement temperature of 25 °C, the temperature optimum of V_{cmax} ($T_{opt,Vcmax}$), the maximum value of V_{cmax} ($k_{opt,Vcmax}$), and the activation energy of V_{cmax} ($H_{a,Vcmax}$) of four southern pine species and related populations. Values marked with * demonstrate a significant positive correlation to the average growth temperature of the thirty days prior to measurement ($T_{growth,30}$), and values marked with ** demonstrate a significant negative correlation to $T_{growth,30}$ ($p < 0.05$).

		V_{cmax}			
Species	Population	$V_{cmax,25}$ (μmol m^{-2} s^{-1})	$T_{opt,Vcmax}$ (° C)	$k_{opt,Vcmax}$ (μmol m^{-2} s^{-1})	$H_{a,Vcmax}$ (kJ mol^{-1})
All		77.20 ± 2.73*	33.46 ± 0.36*	118.33 ± 5.35*	76.80 ± 3.52**
Longleaf		68.15 ± 7.47	34.70 ± 0.72	120.69 ± 10.03	72.33 ± 6.71
	Alabama	71.53 ± 6.98	34.33 ± 1.08	116.09 ± 9.83	65.27 ± 8.45
	Florida	69.44 ± 8.81	35.17 ± 1.66	122.46 ± 28.23	70.14 ± 13.51
	N. Carolina	63.67 ± 8.35*	34.72 ± 1.20	123.97 ± 16.46	81.04 ± 13.34
Loblolly		80.80 ± 6.51*	32.87 ± 0.65	119.72 ± 9.35	75.87 ± 6.00
	Alabama	91.36 ± 12.38	33.98 ± 1.28	141.06 ± 20.83	70.33 ± 6.24
	Arkansas	69.44 ± 9.25	32.27 ± 0.89	97.62 ± 11.81	71.03 ± 11.67
	Florida	82.48 ± 10.91	33.36 ± 1.45*	140.87 ± 20.31	87.48 ± 15.56
	Georgia	81.00 ± 11.27	31.29 ± 1.89*	89.40 ± 12.85	74.66 ± 13.92
Shortleaf		77.34 ± 7.26	32.95 ± 0.74	113.56 ± 14.37*	85.61 ± 7.52
	Arkansas	84.68 ± 8.43	34.06 ± 0.78	136.61 ± 31.06	75.30 ± 11.97
	Mississippi	74.96 ± 15.05*	32.33 ± 1.53	104.50 ± 18.11	91.33 ± 13.91
	Texas	68.29 ± 5.02	32.14 ± 1.53	91.18 ± 18.52	92.93 ± 13.31
Slash		84.57 ± 7.66	33.14 ± 0.76	117.17 ± 10.96	76.67 ± 8.49
	Florida	91.02 ± 10.23	34.81 ± 1.31	142.06 ± 19.00	67.71 ± 11.11
	Georgia	73.60 ± 8.40	33.53 ± 1.14	102.15 ± 16.48	79.56 ± 16.90
	Louisiana	90.23 ± 13.66	31.02 ± 1.34*	109.18 ± 21.04	82.39 ± 16.23

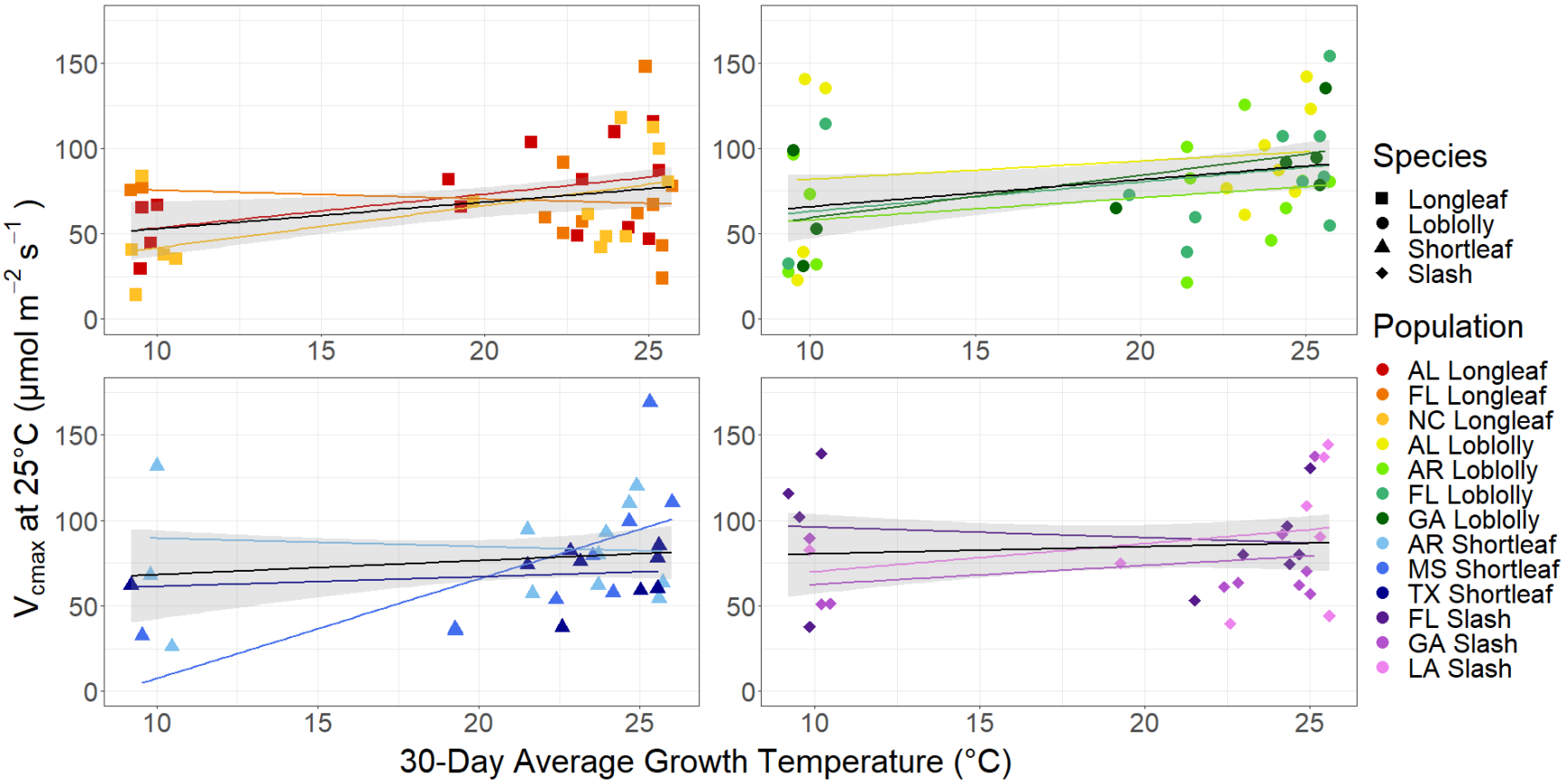

Figure 3. Population-level variation in the maximum velocity of RuBP carboxylation ($V_{cmax,25}$) at a measurement temperature of 25 °C compared to the average growth temperature for the 30 days prior to measurement ($T_{growth,30}$) for four southern pine species and related populations. Solid lines represent linear models fit by population (color) and species (black).

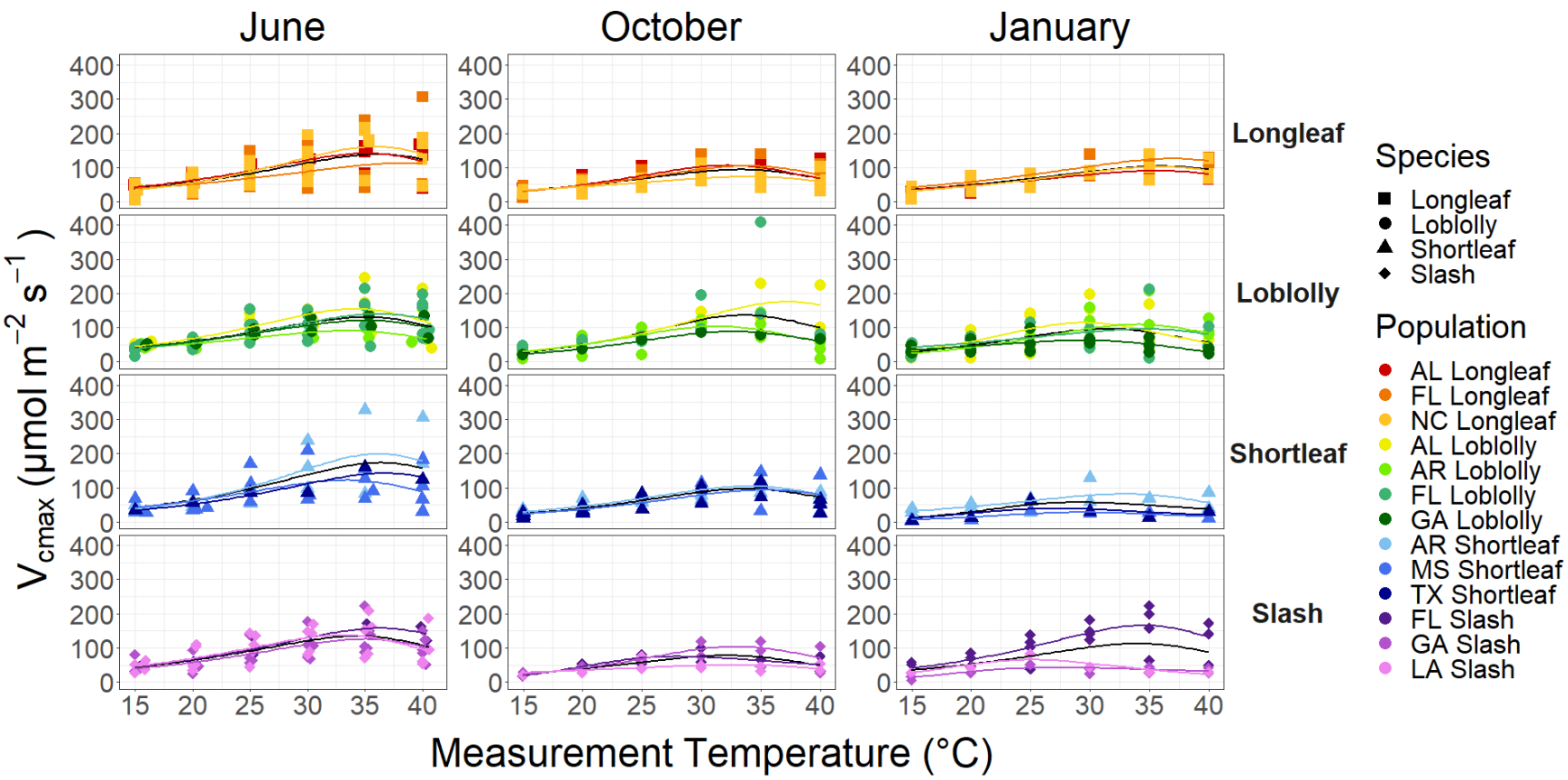

Figure 4. Population-level variation in the maximum velocity of RuBP carboxylation (V_{cmax}) compared to measurement temperature ($T_{measurement}$) across three measurement campaign months for four southern pine species and related populations. Solid lines represent peaked Arrhenius models of V_{cmax} fit by species (black) and population (color).

Temperature Responses of Photosynthetic Parameters: RuBP Regeneration Limitations (J_{max})

No significant differences in the maximum velocity of RuBP regeneration at a measurement temperature of 25 °C ($J_{max,25}$) or in the response of $J_{max,25}$ to $T_{growth,30}$ were exhibited between species or populations (Table 4; $p > 0.05$). When all species and populations were grouped for analysis, no significant relationship was observed between $J_{max,25}$ and $T_{growth,30}$ (Figure 5; $p > 0.05$). No significant differences in the average temperature optimum of J_{max} ($T_{opt,Jmax}$) or in the response of $T_{opt,Jmax}$ to $T_{growth,30}$ were observed at the species or population level (Table 4; $p > 0.05$). When grouped for analysis, the $T_{opt,Jmax}$ for all species and populations increased by 0.17 °C (± 0.052 SE) for each 1 °C increase in $T_{growth,30}$ (Figure 6; $p = 0.0016$). The maximum value of J_{max} ($k_{opt,Jmax}$) also behaved similarly across groups, with no significant differences in the value of $k_{opt,Jmax}$ or in the response of $k_{opt,Jmax}$ to $T_{growth,30}$ observed at the species or population level (Table 3; $p > 0.05$). The mean value of $k_{opt,Jmax}$ across species and populations increased by 2.03 μmol m^{-2} s^{-1} (± 0.78 SE) for each 1 °C increase in $T_{growth,30}$ (Figure 6; $p = 0.0098$). Finally, no significant differences were observed in the average value of the activation energy of J_{max} ($H_{a,Jmax}$) between species and populations ($p > 0.05$). No significant differences were observed in the response of $H_{a,Jmax}$ to $T_{growth,30}$ at the species or population level, and when species and populations were grouped for analysis, no significant relationship was observed between $H_{a,Jmax}$ and $T_{growth,30}$ (Table 4; $p > 0.05$). Like V_{cmax}, the trends for J_{max} were similar across species and populations. As $T_{growth,30}$ increased, the values of $T_{opt,Jmax}$ and $k_{opt,Jmax}$ also increased significantly, although $H_{a,Jmax}$ and $J_{max,25}$ demonstrated no significant relationship to $T_{growth,30}$ when all species and populations were grouped for analysis.

Table 4. Means (± standard error) of the maximum velocity of RuBP regeneration ($J_{max,25}$) at a measurement temperature of 25 °C, the temperature optimum of J_{max} ($T_{opt,Jmax}$), the maximum value of J_{max} ($k_{opt,Jmax}$), and the activation energy of J_{max} ($H_{a,Jmax}$) of four southern pine species and related populations. Values marked with * demonstrate a significant positive correlation to the average growth temperature of the thirty days prior to measurement ($T_{growth,30}$), and values marked with ** demonstrate a significant negative correlation to $T_{growth,30}$ ($p < 0.05$).

		J_{max}			
Species	Population	$J_{max,25}$ (μmol m^{-2} s^{-1})	$T_{opt,Jmax}$ (° C)	$k_{opt,Jmax}$ (μmol m^{-2} s^{-1})	$H_{a,Jmax}$ (kJ mol^{-1})
All		105.47 ± 3.61	31.12 ± 0.35*	128.20 ± 5.14*	39.49 ± 2.76
Longleaf		105.14 ± 7.47	32.66 ± 0.59	146.98 ± 10.25	43.00 ± 5.48
	Alabama	114.55 ± 10.21	31.95 ± 0.75	144.93 ± 11.17	34.69 ± 5.50
	Florida	105.17 ± 16.53	32.89 ± 0.88	140.56 ± 26.56	48.23 ± 15.17
	N. Carolina	95.70 ± 12.72	33.20 ± 1.33	153.84 ± 17.98	47.38 ± 8.63
Loblolly		108.75 ± 6.51*	30.53 ± 0.64*	121.90 ± 7.22	34.90 ± 4.01
	Alabama	118.86 ± 15.89	31.66 ± 1.34	139.60 ± 16.12	42.40 ± 4.62
	Arkansas	94.45 ± 10.56	30.06 ± 0.67	103.85 ± 11.25	25.34 ± 5.10
	Florida	113.94 ± 13.00	30.73 ± 1.66	135.68 ± 13.94	41.46 ± 12.13
	Georgia	109.18 ± 11.90	29.20 ± 1.46*	102.52 ± 11.32	29.00 ± 6.31
Shortleaf		95.60 ± 7.26	30.90 ± 0.70	116.63 ± 15.44*	47.64 ± 7.43
	Arkansas	118.44 ± 10.97	31.39 ± 1.08	149.38 ± 32.31	31.79 ± 8.32
	Mississippi	66.99 ± 11.49	30.54 ± 1.05	101.42 ± 20.21	54.65 ± 13.37
	Texas	88.69 ± 9.01	30.68 ± 1.92	88.56 ± 14.76	61.79 ± 17.18
Slash		112.30 ± 7.66	30.16 ± 0.79	122.43 ± 9.61	34.83 ± 6.05
	Florida	129.89 ± 11.62	30.83 ± 1.28	138.15 ± 14.26	36.18 ± 7.67
	Georgia	97.37 ± 11.16	29.74 ± 1.26	106.28 ± 13.40	43.10 ± 14.98**
	Louisiana	108.98 ± 16.71	29.96 ± 1.71*	124.88 ± 21.84	24.16 ± 4.16

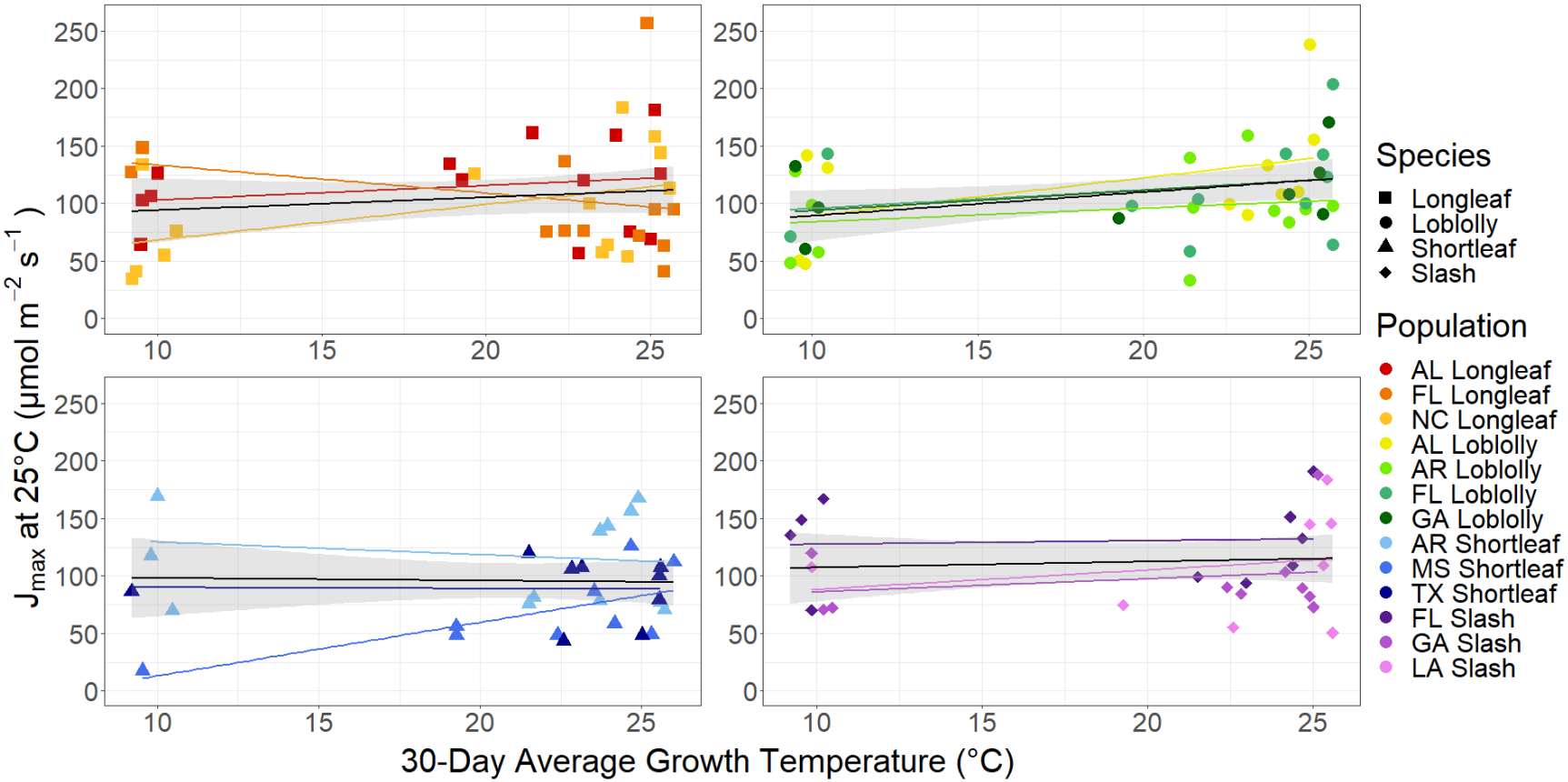

Figure 5. Population-level variation in the maximum velocity of RuBP regeneration ($J_{max,25}$) at a measurement temperature of 25 °C compared to the average growth temperature for the 30 days prior to measurement ($T_{growth,30}$) for four southern pine species and related populations. Solid lines represent linear models fit by population (color) and species (black).

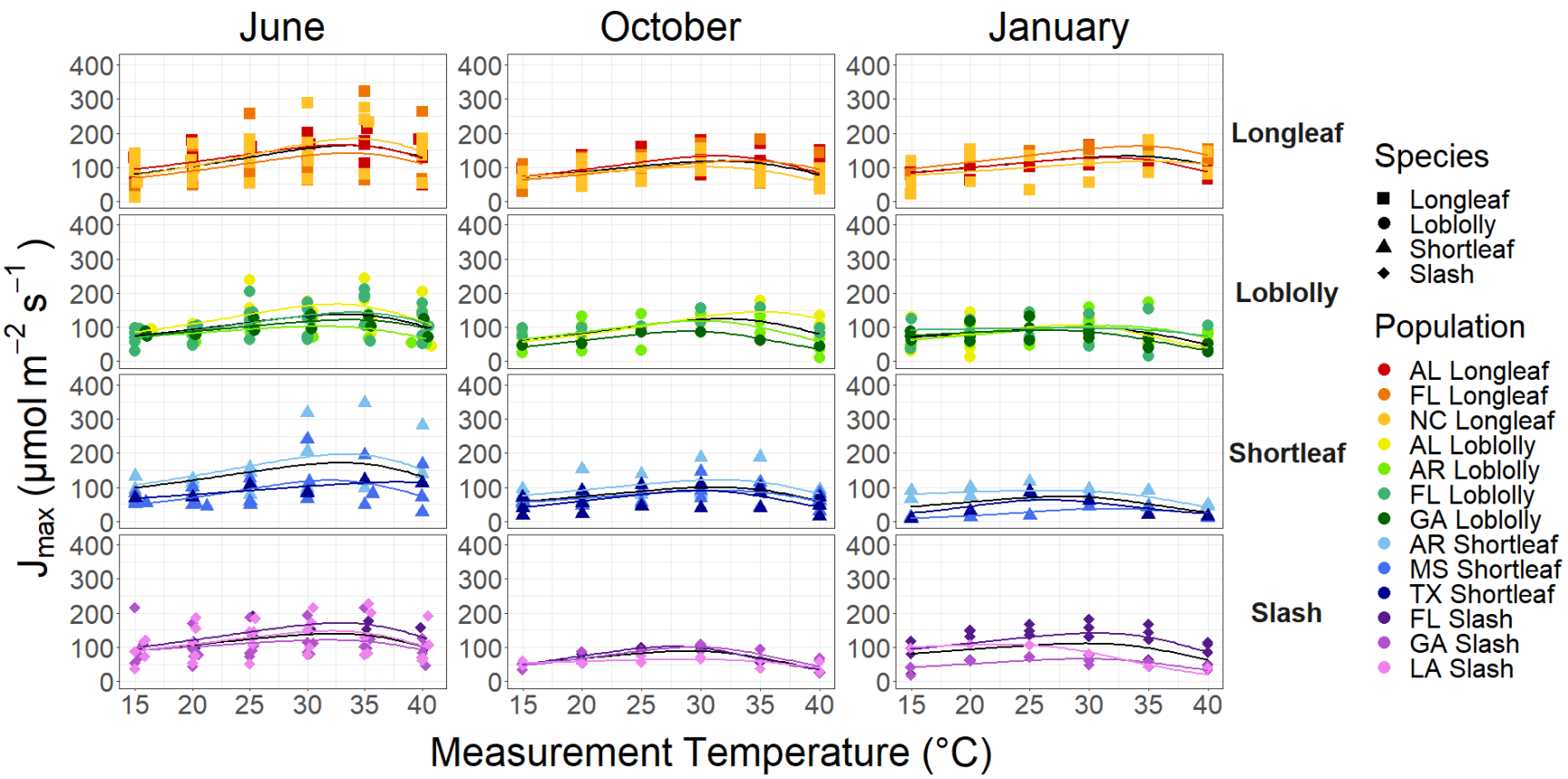

Figure 6. Population-level variation in the maximum velocity of RuBP regeneration (J_{max}) compared to measurement temperature ($T_{measurement}$) across three measurement campaign months for four southern pine species and related populations. Solid lines represent peaked Arrhenius models of J_{max} fit by species (black) and population (color).

Temperature Responses of Photosynthetic Parameters: the Ratio of RuBP Regeneration to RuBP Carboxylation (J_{max} to V_{cmax})

The ratio of $J_{max,25}$ to $V_{cmax,25}$ was found to vary significantly between species ($p = 0.018$). The mean ratio of $J_{max,25}$ to $V_{cmax,25}$ for longleaf pine was 1.57 units (± 0.057 SE), which was found to be significantly higher than mean ratio of $J_{max,25}$ to $V_{cmax,25}$ for shortleaf pine ($p = 0.0031$) and slash pine (Table 2; $p = 0.031$). In contrast, no significant differences were found in the ratio of $J_{max,25}$ to $V_{cmax,25}$ between populations ($p > 0.05$). No significant differences in the temperature response of the ratio of $J_{max,25}$ to $V_{cmax,25}$ to $T_{growth,30}$ were observed between species or populations ($p > 0.05$). When all species and populations were grouped for analysis, the ratio of $J_{max,25}$ to $V_{cmax,25}$ decreased by 0.018 units (± 0.0043 SE) for each 1 °C increase in $T_{growth,30}$ (Figure 7; $p < 0.0001$). Unlike other metrics of net photosynthesis, southern pine species show significant evidence of variation in the ratios of $J_{max,25}$ to $V_{cmax,25}$. However, despite differences in the mean $J_{max,25}$ to $V_{cmax,25}$ ratio between species, the temperature response of the ratio of $J_{max,25}$ to $V_{cmax,25}$ was similar across all species and populations. These findings reflect an overall pattern of similarities in photosynthetic acclimation to temperature for all assessed southern pine species and populations.

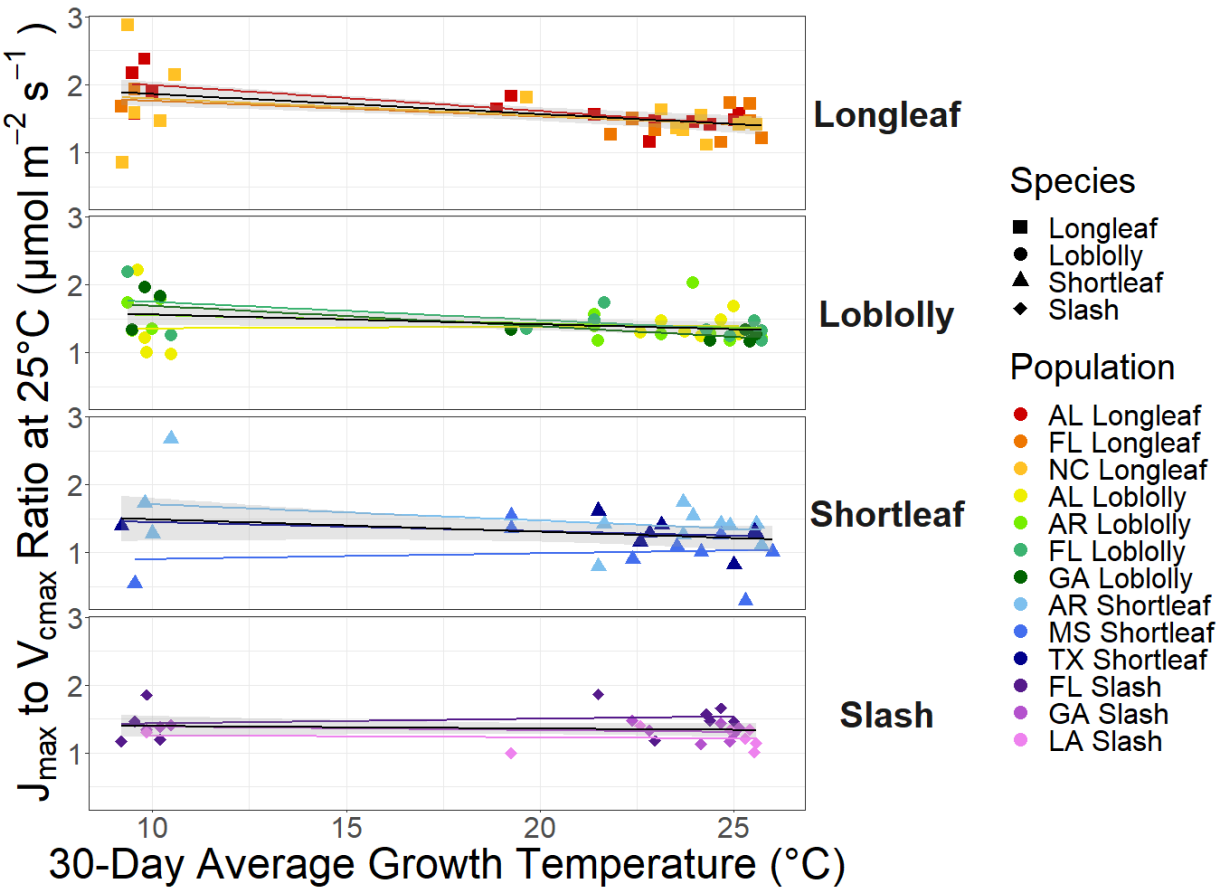

Figure 7. Population-level variation in the ratio of the maximum velocity of RuBP regeneration (J_{max}) to RuBP carboxylation (V_{cmax}) compared to the average growth temperature for the 30 days prior to measurement ($T_{growth,30}$) for four southern pine species and related populations. Solid lines represent linear models fit by population (color) and species (black).

Temperature Responses of Dark Respiration

The respiratory rate when measured in the dark at a fixed temperature of 25 °C (R_{25}) was found to vary significantly between species ($p < 0.0001$), with all species-level comparisons demonstrating significant differences in R_{25} ($p < 0.05$) except the longleaf and slash pine comparison (Table 5; $p = 0.50$). Additionally, species exhibited significant differences in the relationship between R_{25} and $T_{growth,30}$ ($p = 0.010$). For each 1 °C increase in $T_{growth,30}$, the R_{25} of loblolly pine decreased by 0.080 μmol g^{-1} s^{-1} (± 0.030 SE; Figure 8; $p = 0.0069$); no other species exhibited a significant relationship between R_{25} and $T_{growth,30}$ ($p > 0.05$). Although significant differences in the value of R_{25} were present between populations of different species ($p < 0.0001$), no significant differences in R_{25} were found between populations of a given species ($p > 0.05$). There were also no significant differences in the relationship between R_{25} and $T_{growth,30}$ among populations ($p < 0.05$).

Significant species-level differences were found for the rate of respiratory increase per 1 °C increase in measurement temperature at a measurement temperature of 25 °C ($Q_{10,25}$; $p < 0.0001$). Post-hoc analysis revealed a significant difference in the $Q_{10,25}$ values between slash and longleaf pine ($p = 0.0008$) and slash and loblolly pine ($p < 0.0001$), but no other species-level comparisons were statistically significant (Table 5; $p > 0.05$). Significant species-level differences were also found for the relationship between $Q_{10,25}$ and $T_{growth,30}$ ($p < 0.0001$). Only longleaf pine demonstrated a significant relationship between $Q_{10,25}$ and $T_{growth,30}$, where the value of $Q_{10,25}$ decreased by 0.0084 units (± 0.0038 SE) for each 1 °C increase in $T_{growth,30}$ (Figure 11; $p = 0.026$). Significant population-level differences were found for the value of $Q_{10,25}$ ($p < 0.0001$) and the relationship between $Q_{10,25}$ and $T_{growth,30}$ ($p < 0.0001$), although post-hoc tests found no significant comparisons between populations of a given species ($p > 0.05$).

Significant variation in the average value of the coefficient describing the steepness of the short-term respiratory response to temperature (log polynomial parameter *b*) was present at the species level ($p = 0.0002$). Post-hoc analysis revealed significant differences in the value of parameter *b* between longleaf and shortleaf pine ($p = 0.0023$), longleaf and slash pine ($p = 0.040$), and loblolly and shortleaf pine ($p = 0.043$); all other comparisons were non-significant (Table 5; $p > 0.05$). Significant species-level variation was also present in the relationship between parameter *b* and $T_{growth,30}$ ($p < 0.0001$). For each 1 °C increase in $T_{growth,30}$, the value of parameter *b* for shortleaf pine decreased by 0.0023 units (± 0.0009 SE; $p = 0.014$), and the value

of parameter *b* for slash pine increased by 0.0025 units (± 0.0009 SE; $p = 0.0083$). No other species exhibited a significant relationship between log polynomial parameter *b* and $T_{growth,30}$ (Figure 9; $p > 0.05$). Significant population-level differences were also present in the value of log polynomial parameter *b* ($p < 0.0001$) and in the relationship between parameter *b* and $T_{growth,30}$ ($p < 0.0001$), but post-hoc analysis revealed no significant comparisons between populations of the same species (Figure 10; $p > 0.05$).

The coefficient describing the curvature of the short-term respiratory response to temperature (log polynomial parameter *c*) exhibited a complementary pattern to log polynomial parameter *b*. Significant species-level differences were present in the value of log polynomial parameter *c* ($p = 0.0006$) and in the relationship between parameter *c* and $T_{growth,30}$ (Table 5; $p < 0.0001$). Post-hoc analysis revealed a significant difference in the value of parameter *c* between longleaf and shortleaf pine ($p = 0.0006$), but not between any other species ($p > 0.05$). For each 1 °C increase in $T_{growth,30}$, the value of parameter *c* for shortleaf pine increased by 3.86×10^{-5} units ($\pm 1.6 \times 10^{-5}$ SE; $p = 0.017$), and the value of parameter *c* for slash pine decreased by 4.29×10^{-5} units ($\pm 1.6 \times 10^{-5}$ SE; $p = 0.0074$). No other species exhibited a significant relationship between log polynomial parameter *c* and $T_{growth,30}$ (Figure 9; $p > 0.05$). Significant population-level differences were also present in the value of log polynomial parameter *c* ($p < 0.0001$) and in the relationship between parameter *c* and $T_{growth,30}$ ($p < 0.0001$), although post-hoc analysis did not uncover any significant comparisons between populations (Figure 10; $p > 0.05$).

The intercept of the respiratory temperature response curve (log polynomial parameter *a*) was found to vary significantly between all species ($p < 0.05$), with the exception of the comparison between loblolly and longleaf pine and the comparison between loblolly and slash pine (Table 5; $p > 0.05$). The relationship between $T_{growth,30}$ and log polynomial parameter *a* also varied significantly between species ($p = 0.0006$), with only slash pine demonstrating a significant decrease in the value of parameter *a* with increasing $T_{growth,30}$ at the species level ($p = 0.028$). However, when parameter *a* was compared between measurement campaign months, the values of log polynomial parameter *a* for loblolly pine formed a gradient from the highest intercept in January, through October, August, and December to the lowest intercept in June. The mean value of log polynomial parameter *a* for loblolly pine in January was found to be 0.60 $\mu mol\ g^{-1}\ s^{-1}$ (± 0.056 SE) greater than the value of parameter *a* in June ($p = 0.0030$). At the population level, the relationship of log polynomial parameter *a* to $T_{growth,30}$ varied significantly

between populations ($p < 0.0001$), but post-hoc analysis revealed no significant differences in the value of parameter *a* between populations of a given species ($p > 0.05$). For each 1 °C increase in $T_{growth,30}$, the Georgia population of loblolly pine demonstrated a 0.058 μmol g^{-1} s^{-1} (± 0.020 SE) decrease in the value of log polynomial parameter *a* ($p = 0.0037$), and the Louisiana population of slash pine demonstrated a 0.048 μmol g^{-1} s^{-1} (± 0.019 SE) decrease in the value of parameter *a* ($p = 0.012$). In contrast, the value of log polynomial parameter *a* for the Mississippi population of shortleaf pine increased by 0.080 μmol g^{-1} s^{-1} (± 0.021 SE) for each 1 °C increase in $T_{growth,30}$ ($p < 0.001$); no other population demonstrated a significant relationship between parameter *a* and $T_{growth,30}$ ($p > 0.05$).

Most metrics of dark respiration demonstrated both species-level differentiation and variation with increasing $T_{growth,30}$. As $T_{growth,30}$ increased, loblolly pine demonstrated decreasing values of R_{25}, longleaf pine demonstrated decreasing values of $Q_{10,25}$, and slash and shortleaf pine demonstrated opposing patterns of variation in log polynomial parameters *b* and *c*. Finally, species-level variation was evident in the mean values of R_{25} and $Q_{10,25}$, while the shape of the temperature response curve captured by the log polynomial parameters demonstrated evidence of both genetic differentiation and a significant acclimatory relationship to $T_{growth,30}$ at a species and a population level.

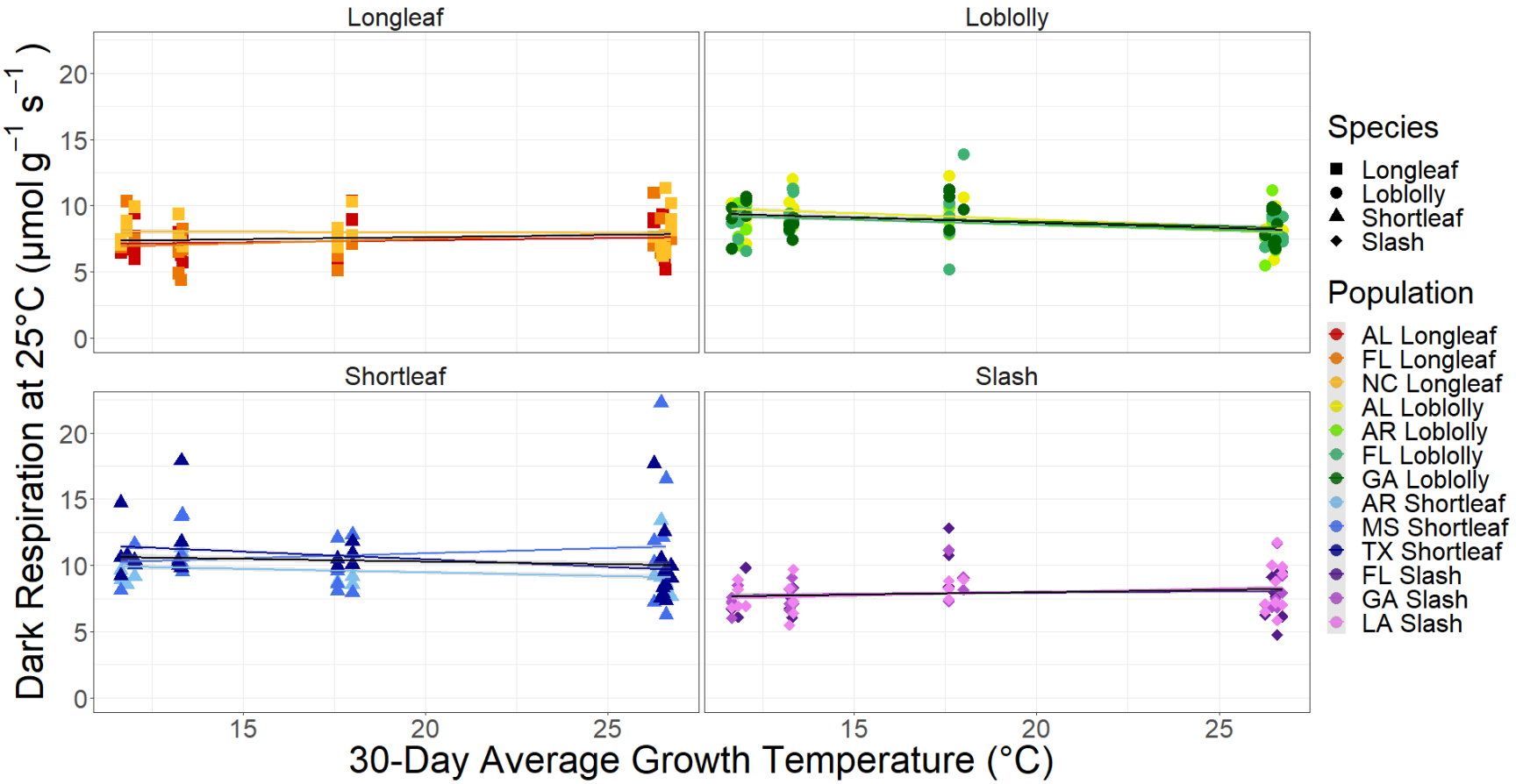

Figure 8. Population-level variation in respiration measured in the dark at 25 °C (R_{25}) compared to the average growth temperature during the 30 days prior to measurement ($T_{growth,30}$) for four southern pine species and related populations. Solid lines represent linear models fit by population (color) and species (black).

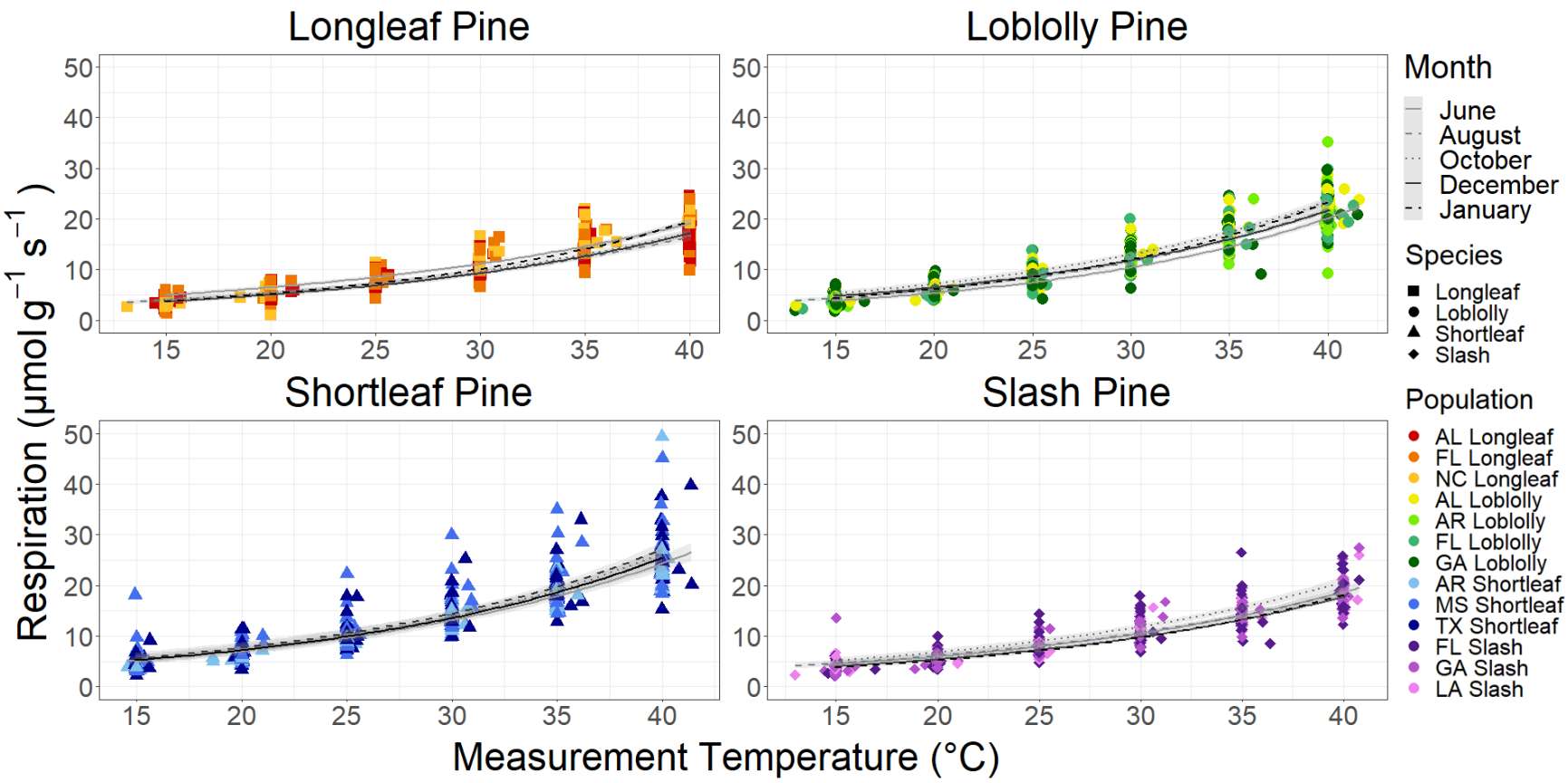

Figure 9. Species-level variation in respiration (R_{dark}) compared to the measurement temperature ($T_{measurement}$) for four southern pine species. Solid lines represent pseudoexponential models of the temperature response of respiration based on log polynomial models fit by campaign month for each species.

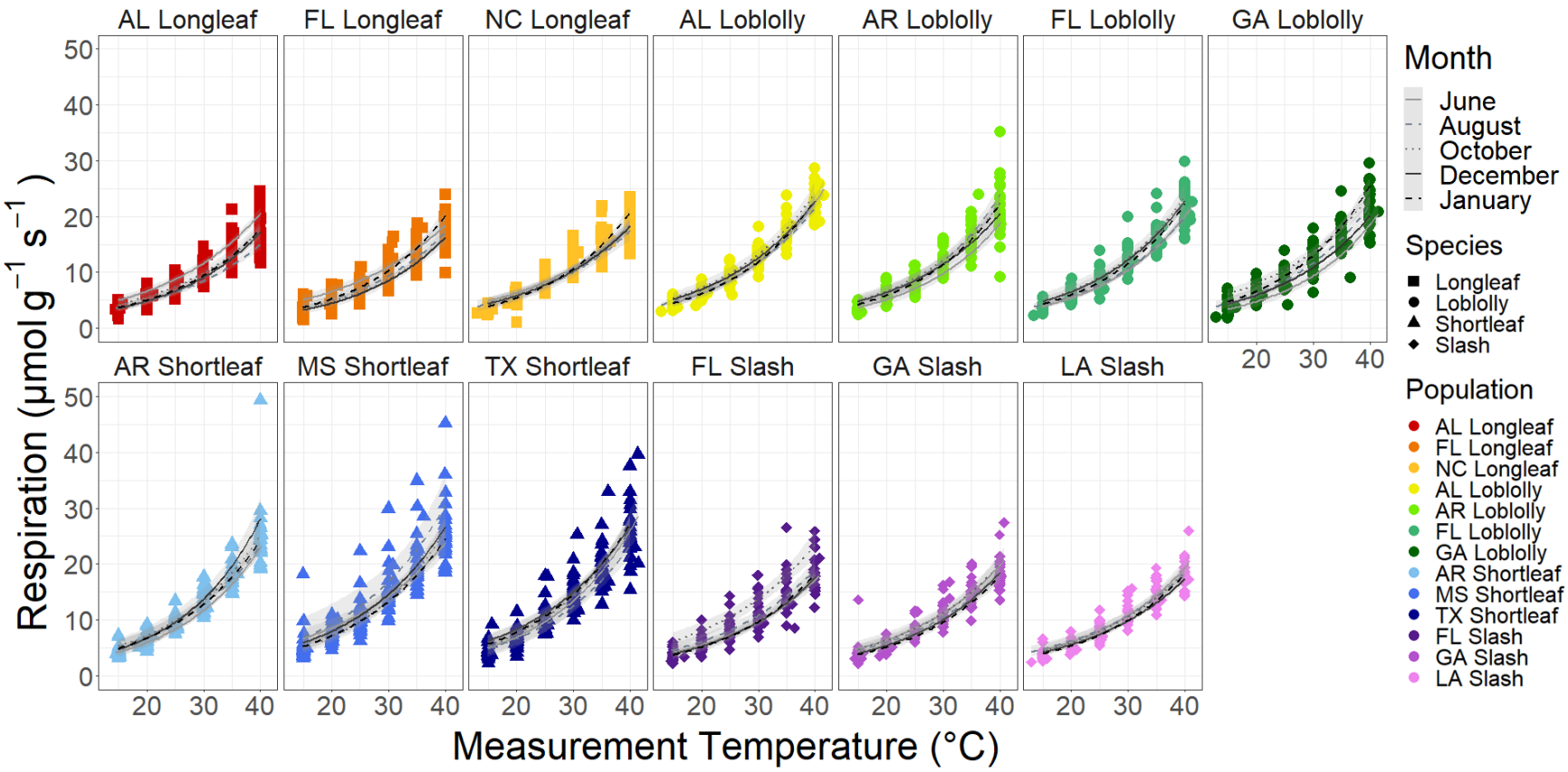

Figure 10. Population-level variation in respiration (R_{dark}) compared to the measurement temperature ($T_{measurement}$) for four southern pine species. Solid lines represent pseudoexponential models of the temperature response of respiration, based on the log polynomial model calculated for each species.

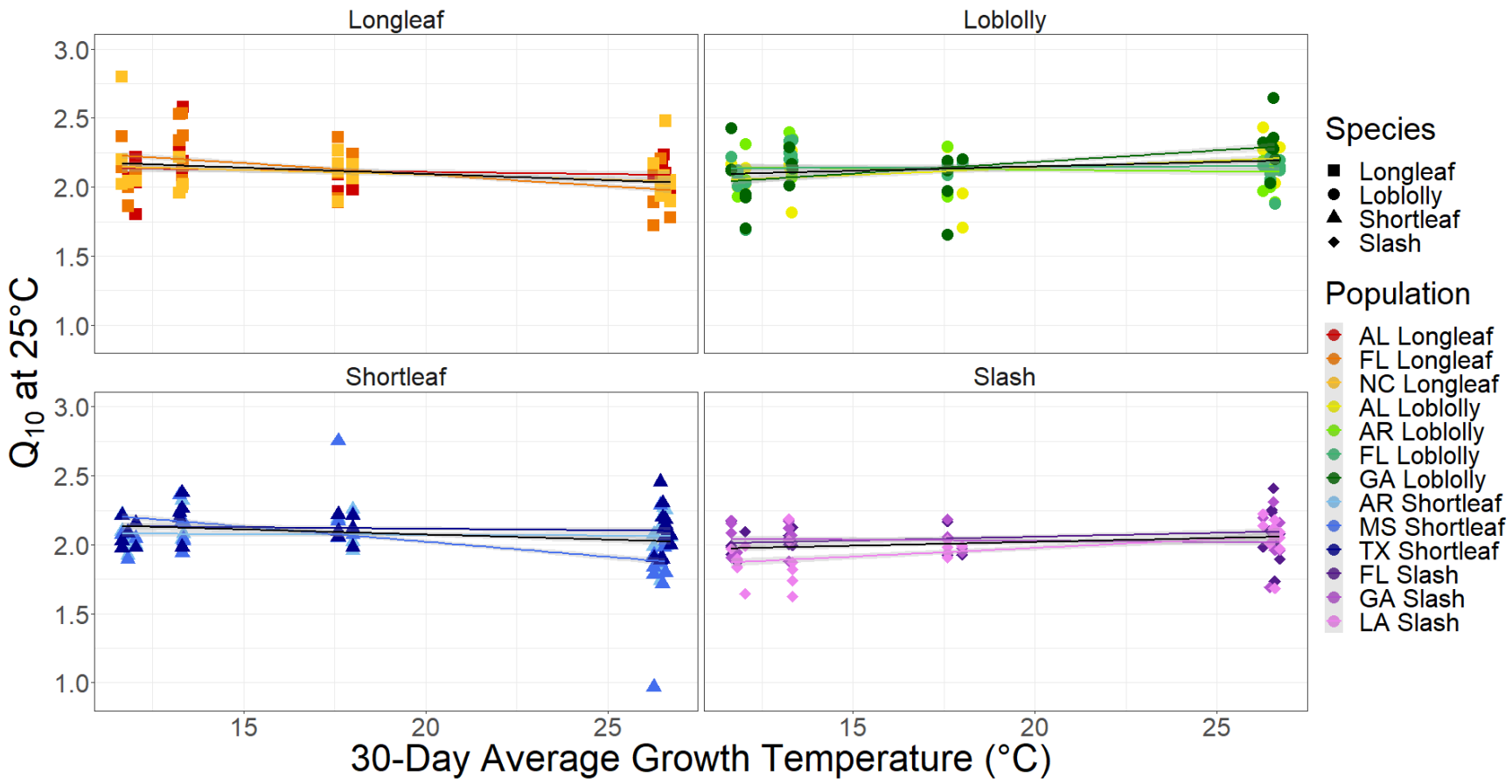

Figure 11. Population-level variation in the rate of respiratory increase per 10 °C increase in measurement temperature (Q_{10}) compared to the average growth temperature during the 30 days prior to measurement ($T_{growth,30}$) for four southern pine species and related populations. Solid lines represent linear models fit by species (black) and population (color).

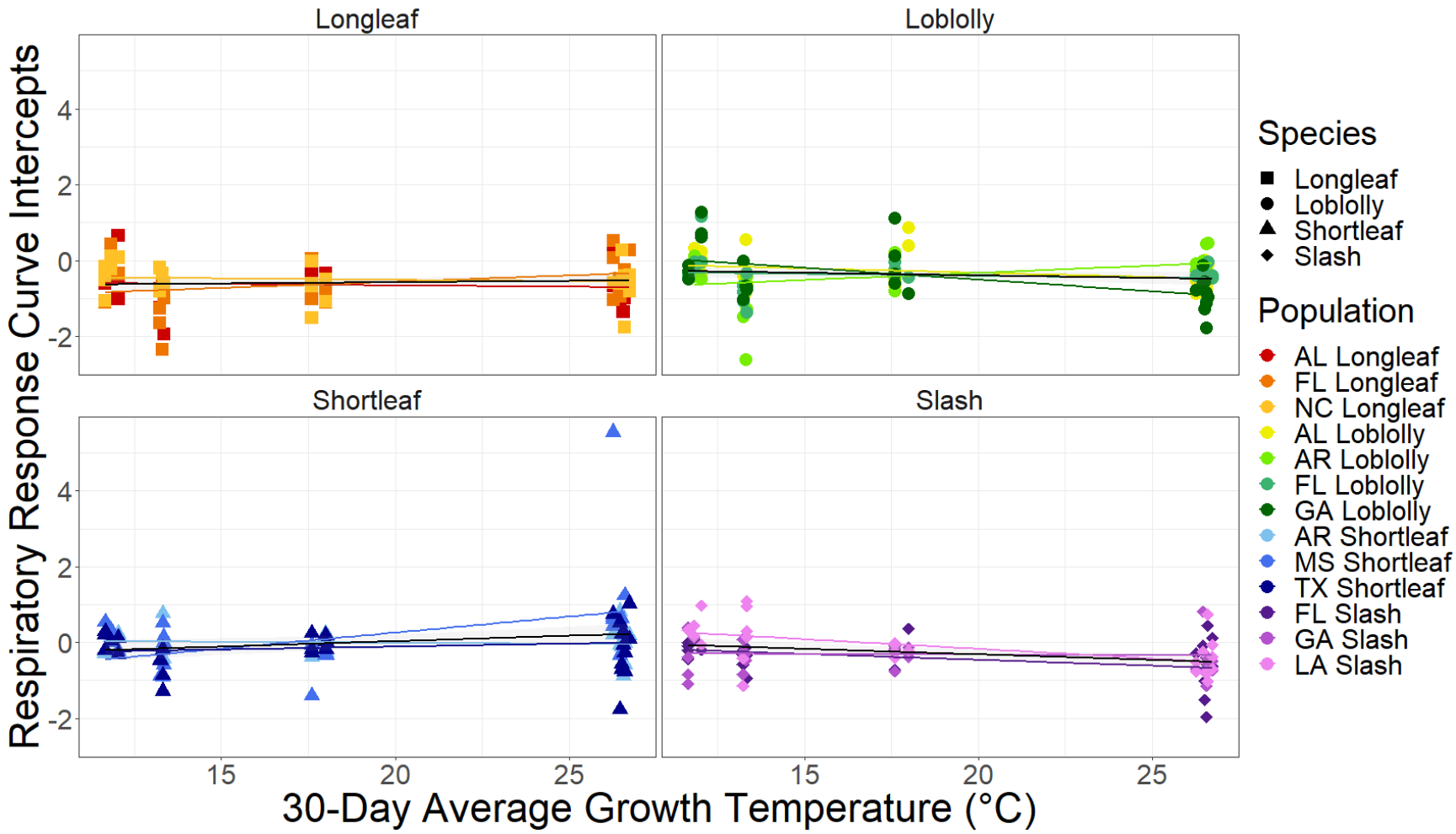

Figure 12. Population-level variation in the intercepts of the respiratory temperature response curves compared to the average growth temperature during the 30 days prior to measurement ($T_{growth,30}$) for four southern pine species and related populations. Solid lines represent linear models fit by species (black) and population (color).

Values of $R_{realized}$ at T_{growth}

Realized respiration ($R_{realized}$) refers to the rate of dark respiration predicted for the average temperature measured in the field on the date of measurement (T_{growth}) based on previously calculated measurements of R_{dark} and values of Q_{10}. Values of $R_{realized}$ were found to vary significantly between species (Table 5; $p < 0.0001$), and the values of $R_{realized}$ were significantly different between all species ($p < 0.001$), with the exception of longleaf and slash pine ($p = 0.61$). No significant relationships were observed between $R_{realized}$ and T_{growth} for any species ($p > 0.05$), and no significant species-level differences were observed in the response of $R_{realized}$ to T_{growth} (Figure 13; $p > 0.05$). Values of $R_{realized}$ were also found to vary significantly between populations ($p < 0.0001$), although post-hoc analysis did not uncover any populations within the same species that had values of $R_{realized}$ that varied significantly from one another ($p > 0.05$). No significant relationships were observed between $R_{realized}$ and T_{growth} for any population ($p > 0.05$), and no significant population-level differences were observed in the response of $R_{realized}$ to T_{growth} ($p > 0.05$). In summary, while mean values of $R_{realized}$ varied between species, all assessed southern pine species and populations demonstrated substantial evidence of respiratory acclimation to temperature, exemplified by near-complete homeostasis in $R_{realized}$ across a broad range of seasonal temperature variation.

Table 5. Means (± standard error) of the predicted rate of dark respiration ($R_{realized}$) for the average growth temperature on the date of measurement (T_{growth}), the measured rate of dark respiration ($R_{dark,25}$), the rate of respiratory increase per 1 °C increase in measurement temperature ($Q_{10,25}$) at a measurement temperature of 25 °C, and the value of the coefficients describing the slope (log polynomial parameter *b*), curvature (log polynomial parameter *c*), and intercept (log polynomial parameter *a*) of the respiratory temperature response curve of four southern pine species and related populations. Values marked with * demonstrate a significant positive correlation to the average growth temperature of the thirty days prior to measurement ($T_{growth,30}$), and ** denotes a significant negative correlation with $T_{growth,30}$ ($p < 0.05$).

		R_{dark}					
Species	Population	$R_{realized}$ ($\mu mol\ g^{-1}\ s^{-1}$)	$R_{dark,25}$ ($\mu mol\ g^{-1}\ s^{-1}$)	$Q_{10,25}$	Log polynomial parameter b	Log polynomial parameter c	Log polynomial parameter a
All		12.81 ± 0.15	8.65 ± 0.11	2.09 ± 0.0098	0.12 ± 0.0024	$-0.00098 \pm 4.02 \times 10^{-5}$	-0.32 ± 0.035
Longleaf		11.18 ± 0.21	7.59 ± 0.15	2.10 ± 0.020**	0.13 ± 0.033	$-0.0012 \pm 6.19 \times 10^{-5}$	-0.58 ± 0.058
	Alabama	10.88 ± 0.37	7.34 ± 0.26	2.11 ± 0.027	0.14 ± 0.0055	$-0.0012 \pm 9.15 \times 10^{-5}$	-0.65 ± 0.093
	Florida	10.90 ± 0.35	7.44 ± 0.29	2.10 ± 0.039	0.13 ± 0.0061	$-0.0011 \pm 9.42 \times 10^{-5}$	-0.58 ± 0.12
	N. Carolina	11.74 ± 0.36	7.98 ± 0.24	2.09 ± 0.034	0.13 ± 0.0070	$-0.0012 \pm 1.32 \times 10^{-4}$	-0.51 ± 0.086
Loblolly		13.20 ± 0.19	8.79 ± 0.14**	2.14 ± 0.016	0.13 ± 0.0039	$-0.0010 \pm 6.86 \times 10^{-5}$	-0.38 ± 0.056
	Alabama	13.71 ± 0.34	8.98 ± 0.28	2.13 ± 0.030	0.13 ± 0.0061	$-0.0010 \pm 1.03 \times 10^{-4}$	-0.31 ± 0.087
	Arkansas	12.86 ± 0.38	8.64 ± 0.33	2.13 ± 0.026	0.13 ± 0.010**	$-0.0010 \pm 1.96 \times 10^{-4}$*	-0.39 ± 0.13
	Florida	12.94 ± 0.45	8.66 ± 0.27	2.14 ± 0.026	0.13 ± 0.0064	$-0.0010 \pm 1.07 \times 10^{-4}$	-0.39 ± 0.090
	Georgia	13.27 ± 0.36	8.86 ± 0.27	2.16 ± 0.042*	0.13 ± 0.0082*	$-0.0011 \pm 1.31 \times 10^{-4}$	-0.43 ± 0.14**
Shortleaf		15.22 ± 0.36	10.30 ± 0.28	2.08 ± 0.024	0.11 ± 0.0064**	$-0.00075 \pm 1.07 \times 10^{-4}$*	0.016 ± 0.092
	Arkansas	14.09 ± 0.38	9.49 ± 0.27	2.07 ± 0.028	0.11 ± 0.0054	$-0.00068 \pm 1.01 \times 10^{-4}$	-0.0082 ± 0.083
	Mississippi	15.97 ± 0.80	10.84 ± 0.61	2.04 ± 0.063**	0.10 ± 0.017**	$-0.00066 \pm 2.76 \times 10^{-4}$*	0.19 ± 0.24*
	Texas	15.47 ± 0.58	10.50 ± 0.46**	2.12 ± 0.025	0.12 ± 0.0075	$-0.00089 \pm 1.36 \times 10^{-4}$	-0.12 ± 0.11
Slash		11.59 ± 0.23	7.93 ± 0.16	2.01 ± 0.017	0.12 ± 0.0046*	$-0.0010 \pm 7.73 \times 10^{-5}$**	-0.29 ± 0.064**
	Florida	11.75 ± 0.46	7.90 ± 0.32	2.05 ± 0.028	0.13 ± 0.0083	$-0.0011 \pm 1.44 \times 10^{-4}$	-0.44 ± 0.11
	Georgia	11.64 ± 0.39	7.97 ± 0.26	2.03 ± 0.028	0.12 ± 0.074	$-0.0010 \pm 1.26 \times 10^{-4}$	-0.32 ± 0.10
	Louisiana	11.39 ± 0.33	7.91 ± 0.27	1.96 ± 0.030*	0.12 ± 0.0076*	$-0.00078 \pm 1.26 \times 10^{-4}$**	-0.12 ± 0.11**

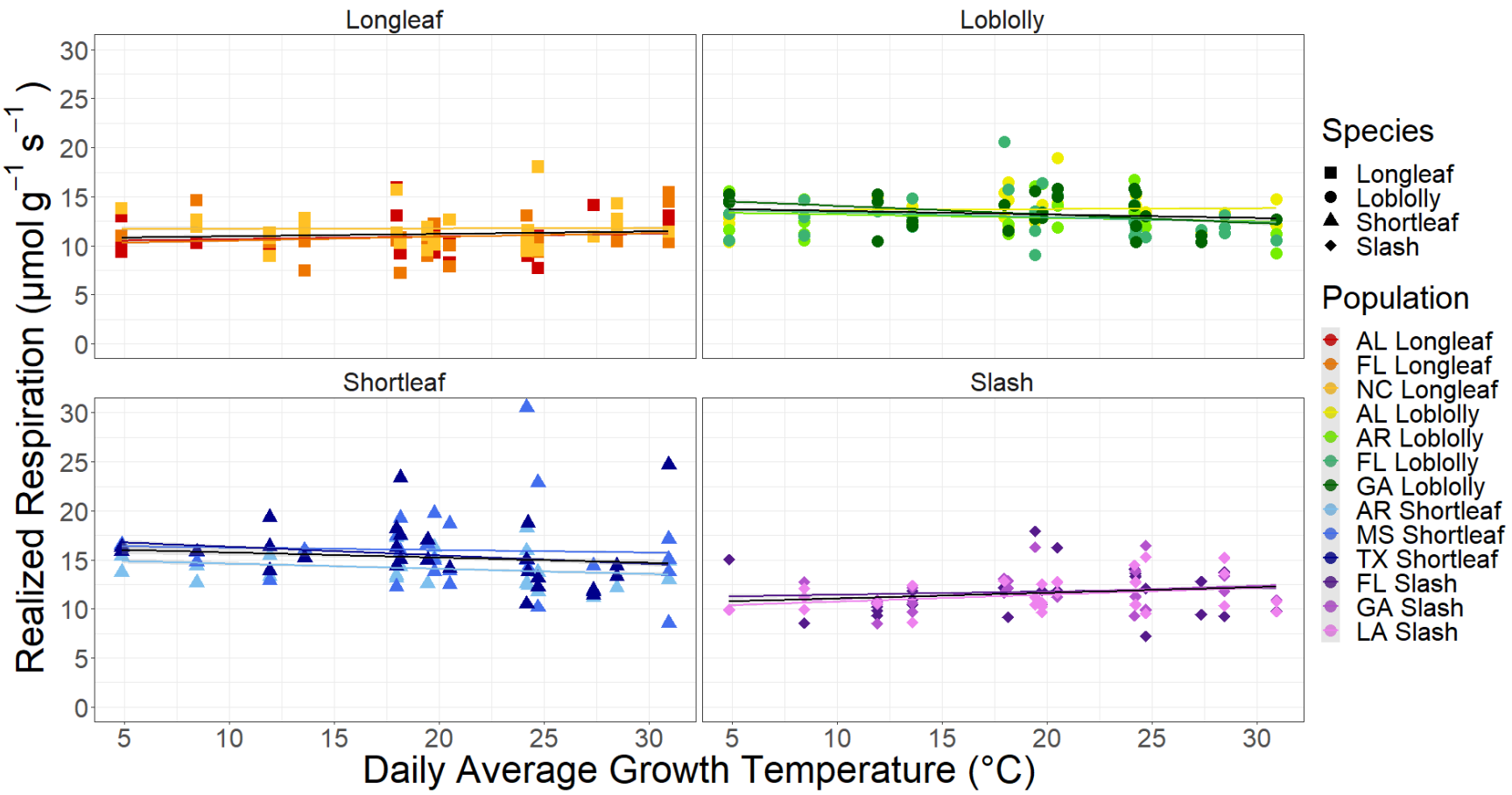

Figure 13. Population-level variation in predicted respiratory rate on the date of measurement ($R_{realized}$) compared to the average growth temperature on the date of measurement (T_{growth}) for four southern pine species and related populations. Solid lines represent linear models fit by species (black) and population (color).

The Ratio of Net Photosynthesis to Dark Respiration

For each 1 °C increase in $T_{growth,30}$, the ratio of $A_{Net,25}$ to R_{25} in longleaf pine increased by 0.049 units (± 0.015 SE; $p = 0.0012$), the ratio of $A_{Net,25}$ to R_{25} in loblolly pine increased by 0.10 units (± 0.014 SE; $p < 0.001$), and the ratio of $A_{Net,25}$ to R_{25} in shortleaf pine increased by 0.071 units (± 0.015 SE; $p < 0.001$); the ratio of $A_{Net,25}$ to R_{25} in slash pine did not demonstrate a significant relationship to $T_{growth,30}$ (Table 2; $p = 0.051$). Significant species- and population-level differences were also observed in the ratio of $A_{Net,25}$ to R_{25} ($p < 0.05$), although post-hoc analysis did not uncover any significant comparisons ($p > 0.05$). Despite similarities in the temperature responses and overall rate of net photosynthesis across species and populations, species-level variation in dark respiration resulted in substantially different ratios of $A_{Net,25}$ to R_{25}, with potential implications for the patterns of carbon flux affected by the balance between these physiological factors.

Growth

The average stem diameter at the root collar (*RCD*) across all destructively sampled individuals at the time of final harvest was 29.53 mm (± 0.40 SE). Values of *RCD* were found to vary significantly between species ($p < 0.0001$) and populations (Table 6; $p = 0.024$). Post-hoc analysis revealed that the average *RCD* values for longleaf, loblolly, and slash pine were significantly larger than that of shortleaf pine ($p < 0.05$), and the average *RCD* of slash pine was significantly larger than that of loblolly pine ($p = 0.017$). All other *RCD* comparisons were non-significant ($p > 0.05$).

The average stem length across all destructively sampled individuals at the time of final harvest was 73.54 cm (± 3.21 SE). Stem lengths varied significantly between species ($p < 0.0001$), but not between populations of a given species ($p > 0.05$). Post-hoc analysis revealed significant differences between the stem lengths of all species ($p < 0.05$). Loblolly pine had the longest average stem lengths, followed by slash, shortleaf, and longleaf pine (Table 6).

The average total dry mass across all destructively sampled individuals at the time of final harvest was 343.53 g (± 10.34 SE). Total, leaf, stem, and root dry masses varied significantly between species ($p < 0.0001$), although only total, leaf, and root dry masses varied significantly between populations (Table 6; $p < 0.05$). With the exceptions of the comparison between slash and loblolly pine and the comparison between shortleaf and longleaf pine ($p > 0.05$), all species demonstrated significant differences in total dry mass ($p < 0.05$). For the mean

value of leaf dry mass, all species-level comparisons were significant ($p < 0.05$), except for the comparison between longleaf and shortleaf pine ($p > 0.05$). At the population level, the North Carolina population of longleaf pine exhibited significantly lower levels of leaf dry mass than the Alabama population of longleaf pine ($p = 0.020$). Similarly, all species demonstrated significant differences in stem dry mass ($p < 0.05$) with the exception of the comparison between loblolly and slash pine ($p > 0.05$). Finally, loblolly, slash, and shortleaf pine all exhibited significantly larger average root dry masses than longleaf pine ($p < 0.05$), and loblolly pine exhibited a significantly larger average root dry mass than shortleaf pine ($p = 0.033$). All other dry mass comparisons were non-significant ($p > 0.05$).

Table 6. Means (± standard error) of root collar diameter, stem length, and dry mass growth metrics at the time of final harvest of four southern pine species and related populations. Superscripts denote statistically significant differences between groups ($p < 0.05$).

Species	Population	Root Collar Diameter (mm)	Stem Length (cm)	Total Dry Mass (g)	Root Dry Mass (g)	Stem Dry Mass (g)	Leaf Dry Mass (g)
Longleaf		29.72 ± 0.87^{b}	16.10 ± 1.06^{d}	222.08 ± 13.02^{b}	96.62 ± 5.88^{c}	20.66 ± 1.60^{c}	104.80 ± 6.81^{c}
	AL	32.75 ± 1.56	19.13 ± 1.70	260.37 ± 20.42	109.61 ± 10.30	24.17 ± 2.87	126.59 ± 10.45^{de}
	FL	28.58 ± 1.05	16.57 ± 1.64	234.62 ± 21.81	78.34 ± 10.52	16.67 ± 2.63	76.24 ± 10.89^{e}
	NC	27.81 ± 1.54	12.60 ± 1.79	171.24 ± 18.55	101.92 ± 8.08	21.13 ± 2.58	11.56 ± 9.64^{ef}
Loblolly		29.37 ± 0.47^{b}	104.71 ± 1.98^{a}	406.67 ± 12.77^{a}	162.67 ± 6.63^{a}	110.48 ± 3.43^{a}	133.53 ± 4.87^{b}
	AL	28.76 ± 0.40	105.05 ± 3.64	363.47 ± 13.60	142.22 ± 7.86	101.01 ± 4.66	120.24 ± 5.16
	AR	29.07 ± 1.07	99.85 ± 4.07	410.57 ± 40.10	165.64 ± 20.90	112.61 ± 10.20	132.33 ± 11.73
	FL	28.95 ± 1.34	105.76 ± 3.12	410.59 ± 20.94	162.52 ± 10.27	114.54 ± 6.64	133.52 ± 9.25
	GA	30.71 ± 0.76	107.77 ± 5.01	445.98 ± 21.55	182.24 ± 11.54	114.71 ± 5.65	149.04 ± 11.57
Shortleaf		24.60 ± 0.87^{c}	68.79 ± 3.23^{c}	272.23 ± 20.38^{b}	131.99 ± 10.04^{b}	56.48 ± 4.64^{b}	83.76 ± 6.72^{c}
	AR	26.00 ± 1.04	67.93 ± 6.22	282.79 ± 38.92	145.57 ± 18.88	55.32 ± 7.29	81.90 ± 13.24
	MS	22.74 ± 1.68	71.68 ± 6.81	246.70 ± 40.88	110.68 ± 17.75	52.40 ± 9.34	83.62 ± 14.25
	TX	25.05 ± 1.61	66.75 ± 4.32	287.22 ± 29.19	139.72 ± 14.73	61.73 ± 8.37	85.76 ± 8.96
Slash		32.02 ± 0.73^{a}	91.80 ± 1.79^{b}	416.42 ± 15.57^{a}	145.03 ± 7.32^{ab}	112.94 ± 4.54^{a}	158.45 ± 5.59^{a}
	FL	31.45 ± 1.59	93.23 ± 3.06	390.02 ± 26.70	128.91 ± 10.38	105.08 ± 7.66	156.03 ± 10.96
	GA	30.40 ± 0.57	93.34 ± 2.99	387.03 ± 19.71	128.12 ± 10.47	109.44 ± 6.02	149.47 ± 7.94
	LA	34.22 ± 1.25	88.83 ± 3.35	472.22 ± 28.09	178.07 ± 12.08	124.28 ± 9.14	169.87 ± 9.75

Discussion

Accurately modeling the acclimation of photosynthesis and photosynthetic parameters has crucial implications for accurately predicting future global carbon feedbacks (Kumarathunge *et al*. 2019), and additional research into the temperature responses of key photosynthetic and respiratory variables have been listed as a major requirement for the improvement of terrestrial biosphere models (Lombardozzi *et al*. 2015; Rogers *et al*. 2017). In order to improve the scientific understanding of physiological temperature responses in southern pine species, we grew three to four geographically distinct populations of loblolly, longleaf, slash, and shortleaf pine in a common garden plot and took measurements of net photosynthesis and dark respiration at set timepoints throughout the study duration. We hypothesized that species from warmer home climates would demonstrate higher photosynthetic and lower respiratory rates than those from cooler home climates. We also hypothesized that species with wider home ranges would demonstrate a greater extent of photosynthetic and respiratory temperature acclimation than those with narrower home ranges. Our analysis revealed no evidence of genetic differentiation or adaptation in net photosynthesis at the species level. In contrast, all four species demonstrated significant evidence of respiratory adaptation and acclimation to temperature. Although all assessed species demonstrated similar extents of photosynthetic acclimation, the mechanism of both photosynthetic and respiratory acclimation varied between species. These findings emphasize that both the extent and the mechanism of photosynthetic and respiratory acclimation must be understood in order to generate accurate predictions of future carbon fluxes.

Net Photosynthesis Responds to Variation in Growth Temperature Similarly Across Species

As none of the assessed species or populations demonstrated significant differences in $A_{Net,25}$ or $T_{opt,A}$, we reject the hypothesis that species and populations from different home climates will demonstrate adaptive differences in photosynthetic rate. These findings are in contrast with a number of studies that found significant evidence of photosynthetic adaptation in *Eucalyptus pauciflora* (Slayter and Ferrar 1977) and *Picea abies* (Oleksyn *et al.* 1998), but are in agreement with Samuelson *et al.* (2012), who found no significant evidence of photosynthetic adaptation in loblolly, longleaf, or slash pine. The wide variation in photosynthetic adaptation trends present in the literature reflects the challenging nature of predicting patterns of photosynthetic adaptation to temperature across forest species. A similar range of findings have been found for assessments of

photosynthetic acclimation to temperature. Significant evidence of photosynthetic acclimation to temperature has been found in *Hevea brasiliensis* (Kositsup *et al.* 2008), *Populus balsamifera* (Silim *et al.* 2010), and some populations of *Corymbia calophylla* (Aspinwall *et al.* 2017b), while *Populus tremuloides*, *Betula papyrifera*, *Populus deltoides*, and *Liquidambar styraciflua* showed minimal evidence of photosynthetic acclimation to temperature across populations (Dillaway and Kruger 2010). Although previous studies have found no evidence of photosynthetic acclimation in mature longleaf and slash pines (Samuelson *et al.* 2012) and conflicting patterns in loblolly pine (Teskey and Will 1999; Samuelson *et al.* 2012), all four species assessed during this experiment demonstrated significant evidence of photosynthetic acclimation to temperature when compared over nearly a full year's range of temperature variation. Additionally, the mechanism of photosynthetic acclimation appeared to vary substantially between longleaf, loblolly, shortleaf, and slash pine.

For longleaf pine, the maintenance of a constant maximum photosynthetic rate was accomplished through subtle changes to the balance between photosynthetic parameters. Although neither $J_{max,25}$ nor $V_{cmax,25}$ demonstrated a significant relationship to $T_{growth,30}$, the ratio of $J_{max,25}$ to $V_{cmax,25}$ decreased significantly as $T_{growth,30}$ increased. While J_{max} and V_{cmax} are often tightly co-regulated, previous studies have found that a decrease in the J_{max} to V_{cmax} ratio results in an increase in the temperature sensitivity of photosynthesis and the $T_{opt,A}$, as J_{max} typically has a higher temperature optimum than V_{cmax} (Onoda *et al.* 2005; Hikosaka *et al.* 2006; Fan *et al.* 2011). In addition, the North Carolina population of longleaf pine demonstrated a significant increase in the value of photosynthetic parameter *b* with $T_{growth,30}$, providing additional evidence of an increase in the temperature sensitivity of photosynthesis with increasing growth temperature. As variation in the value of parameter *b* would capture seasonal changes in the temperature sensitivity of photosynthesis that are not directly connected to RuBP carboxylation or regeneration efficiency, this finding suggests that the North Carolina population of longleaf pine may have access to additional acclimatory strategies that the other populations lack, corresponding to its more seasonal home climate. Therefore, longleaf pine shows substantial evidence of differences in acclimation potential between populations, with evidence of photosynthetic acclimation to temperature increasing with latitude. Additional research into alternative acclimatory mechanisms, such as seasonal adjustments to stomatal regulation or

respiratory rate, may assist in fully understanding population-level differences in the temperature response of net photosynthesis.

Unlike longleaf pine, photosynthetic acclimation for loblolly pine primarily took the form of adjustments to RuBP regeneration efficiency via increases in $J_{max,25}$ and $T_{opt,Jmax}$. An increase in the saturation level of thylakoid membrane lipids is often cited as a major mechanism of photosynthetic acclimation to increases in temperature (Berry and Björkman 1980; Hüve *et al.* 2006; Allakhverdiev *et al.* 2008) and may serve as the biochemical mechanism of acclimation in loblolly pine. Although population-level trends generally reflected species-level trends in photosynthetic acclimation for loblolly pine, the Georgia and Florida populations also demonstrated evidence of acclimation in the temperature optimum of V_{cmax}. Therefore, although all loblolly pine populations demonstrated a similar potential for photosynthetic acclimation via J_{max}, the potential for V_{cmax} acclimation may vary by population, with no clear effect of home climate. These findings are in general agreement with a previous study of photosynthetic acclimation in loblolly pine (Teskey and Will 1999), although significant population-level variation has not previously been detected in this species.

In shortleaf pine, photosynthetic acclimation occurred by increasing the maximum velocities of RuBP carboxylation ($k_{opt,Vcmax}$) and regeneration ($k_{opt,Jmax}$), with minimal population-level variation in acclimatory trends. As photosynthetic acclimation occurred through increases in the values of k_{opt} rather than T_{opt} or activation energy, the biochemical mechanism of acclimation may have primarily involved increasing the concentration of key photosynthetic components, not changing the temperature stability of photosynthetic components. However, increases in leaf-level Rubisco content typically do not result in proportional increases in V_{cmax} or the initial slope of the *A*-*Ci* curve (Yamori *et al.* 2005). Therefore, relying primarily on increases in the concentration of limiting photosynthetic machinery may represent an energetically inefficient acclimatory strategy, where increasing investments in photosynthetic machinery yield diminishing returns in photosynthetic rate. The high energetic cost of this strategy may partially explain why the photosynthetic acclimation of shortleaf pine was unable to overcome the increase in respiratory costs with growth temperature, resulting in a significant decrease in $T_{opt,A}$ with increasing $T_{growth,30}$. Additional research will be required to confirm the biochemical mechanism of photosynthetic acclimation and to fully elucidate the connection between rates of respiration and photosynthesis in shortleaf pine.

Slash pine demonstrated a substantially different mechanism of acclimation from the other three species. For slash pine, photosynthetic acclimation was accomplished through a decrease in the activation energy of RuBP regeneration, causing the rate of photosynthesis for slash pine became more limited by V_{cmax} than J_{max} at elevated growth temperatures. The resulting alteration to the overall shape of the J_{max} curve would have also resulted in an increase the minimum velocity of RuBP regeneration increased with $T_{growth,30}$. This evidence would be consistent with an increased rate of cyclic electron flow along the thylakoid membrane electron transport chain, which some authors have proposed as a potential mechanism of maintaining a sufficient proton gradient for ATP generation under high temperature conditions (Allakhverdiev *et al.* 2008; Sharkey and Zhang 2010). However, similar to shortleaf pine, $T_{opt,A}$ for slash pine also declined significantly with increasing $T_{growth,30}$, implying that the acclimatory strategy employed by slash pine was insufficient to overcome the increase in respiratory costs with an increasing growth temperature. Slash pine also demonstrated substantial evidence of differences in acclimation potential between populations. Unlike other slash pine populations, the Louisiana population of slash pine exhibited significant increases in the of $T_{opt,Vcmax}$ with increasing $T_{growth,30}$. Therefore, the Louisiana population may acclimate to increasing $T_{growth,30}$ through alterations to the activity or efficiency of Rubisco (Berry and Björkman 1980; Sage *et al.* 2008), in a mechanism that is absent in the other assessed populations of slash pine.

Contrary to expectations, species-level patterns of photosynthetic acclimation did not correspond to home range size, with all four species demonstrating a similar extent of photosynthetic acclimation. However, the mechanism of photosynthetic acclimation varied substantially between species. Longleaf pine acclimated through minor adjustments to the balance between RuBP carboxylation and regeneration, while loblolly pine acclimated primarily through alterations to RuBP regeneration efficiency. In contrast, shortleaf pine demonstrated only incomplete acclimation through the modification of $k_{opt,Vcmax}$ and $k_{opt,Jmax}$, and slash pine demonstrated similarly incomplete photosynthetic acclimation through a decrease in $H_{a,Jmax}$ with increasing $T_{growth,30}$. Finally, while the temperature responses of net photosynthesis for most populations within a species did not demonstrate a clear correlation with climate of origin, the North Carolina population of longleaf pine exhibited evidence of acclimatory mechanisms that were absent in the other assessed populations. Therefore, there is some evidence of a climactic influence on the extent of acclimation experienced within populations of longleaf pine. These

findings demonstrate that the extent and mechanism of photosynthetic acclimation is not easily predictable based on a species' climate of origin, in agreement with previous findings (Kumarathunge *et al.* 2019).

Dark Respiration Exhibits Species-Level Adaptation and Acclimation to Growth Temperature

In contrast to net photosynthesis, basal levels of R_{dark} demonstrated substantial variation between southern pine species. The mean values of R_{25} and $R_{realized}$ for the two species with the most southern ranges, longleaf and slash pine, were significantly lower than those of the two species with the most northern ranges, shortleaf and loblolly pine. The lower basal values of R_{dark} in longleaf and slash pine likely reflect lower respiratory maintenance costs (Reich *et al.* 1996), which would be expected to have a more deleterious effect on trees grown at a high temperature than those grown at a low temperature due to the quasi-exponential relationship between respiratory rate and temperature (Atkin and Tjoelker 2003). Therefore, the lower basal values of R_{dark} observed in longleaf and slash pine support our hypothesis that species with more southern home ranges will demonstrate a greater degree of respiratory adaptation to temperature than species with more northern home ranges. Overall, these findings are in agreement with several other studies that found significant differentiation in respiratory rate due to latitude (Reich *et al.* 1996; Quan and Wang 2018) and altitude (Oleksyn *et al.* 1998). However, unlike much of the published literature, we found little population-level evidence of genetic differentiation or adaptation. This result is similar to that of Silim *et al.* (2009), which found minimal evidence of respiratory adaptation among populations of *Populus balsamifera*. Future experiments may aim to repeat this experiment with a different selection of southern pine provenances in order to determine if variation in basal rates of R_{dark} is present among the populations that were not sampled during this study.

R_{dark} also demonstrated considerable variation in response to changes in growth temperature throughout the study duration, with the temperature response of R_{dark} varying substantially between species and populations. Longleaf pine demonstrated clear evidence of Type I acclimation via a decrease in the value of $Q_{10,25}$ as $T_{growth,30}$ increases, resulting in an overall decrease in the responsiveness of R_{dark} to temperature (Atkin and Tjoelker 2003). No significant variation in the temperature response of respiration or in the intercept of the

temperature response curve was observed between populations of longleaf pine, suggesting that population-level variation in the ability of R_{dark} to acclimate may be minimal for longleaf pine.

Loblolly pine demonstrates significant evidence of respiratory acclimation to temperature, as exemplified through a decrease in R_{25} with increasing $T_{growth,30}$. Despite the lack of a significant relationship between $T_{growth,30}$ and log polynomial parameter *a*, the significant difference in parameter *a* between the temperature response curves for January and June suggests that loblolly pine may demonstrate Type II acclimation. The substantially lower intercept of the temperature response curve in June would result in an overall decrease in the basal respiratory rate of loblolly pine at elevated growth temperatures, mitigating the deleterious effects of a pseudo-exponential increase in respiratory rate with temperature (Atkin and Tjoelker 2003). Although most loblolly pine populations did not demonstrate significant shifts in the intercepts of their temperature response curves with increasing $T_{growth,30}$, the Georgia population of loblolly pine exhibited significant evidence of Type II acclimation through a decreasing value of parameter a with increasing $T_{growth,30}$. In contrast, the Arkansas population of loblolly pine exhibited evidence of Type I acclimation through a significant decline in the steepness and increase in the curvature of the respiratory temperature response with increasing growth temperature. Although no other population demonstrated a significant relationship between $T_{growth,30}$ and the temperature response of respiration, the differences in acclimatory trends between loblolly pine populations provides indirect evidence of differences in acclimation potential between populations of loblolly pine. These results are in agreement with those of Teskey and Will (1999), which found significant evidence of population-level differences in acclimation potential among provenances of loblolly pine from Texas, Arkansas, and Maryland. Additional experiments will be required to fully uncover the relationship between differences in acclimation potential and seed source for loblolly pine.

Shortleaf pine demonstrated evidence of Type I respiratory acclimation, which was largely driven by the trend observed in the Mississippi population. As $T_{growth,30}$ increased, the response of respiration to temperature for shortleaf pine became less steep but more curved, leading to the greatest reductions in respiratory rate at low to moderate temperatures. However, this mechanism of Type I acclimation comes with a potential tradeoff, as the rate of respiration would increase rapidly at high measurement temperatures. For this experiment, the elevated temperatures experienced in the field during the warmest months may have been sufficient to

trigger this tradeoff, potentially contributing to the observed decrease in $T_{opt,A}$ with increasing $T_{growth,30}$. As global surface temperatures continue to increase, the potential tradeoff of this acclimatory approach may increase in prominence, to the detriment of the growth and function of affected shortleaf pines. Further research will be required to fully understand the complex interplay between photosynthetic and respiratory responses to temperature, as well as the potential implications for the future conservation of shortleaf pine.

Like shortleaf pine, slash pine demonstrated evidence of Type I respiratory acclimation. Unlike shortleaf pine, however, the temperature response curve for respiration in slash pine became steeper and less curved with increasing $T_{growth,30}$. This pattern of Type I acclimation would reduce the temperature sensitivity of respiration across all temperatures, preventing the rapid increase in respiratory rate experienced by shortleaf pine at high temperatures. Slash pine also demonstrated significant evidence of Type II acclimation, as the intercept of the temperature response curve and corresponding rate of basal respiration decreased significantly with increasing $T_{growth,30}$. The observed trends in slash pine were largely driven by the Louisiana population, although additional research will be required to fully understand population-level differences in acclimation potential for slash pine.

Surprisingly, Type I and Type II acclimation strategies were equally common for the species assessed. While many species in the published literature have been observed to acclimate primarily or exclusively through Type II respiratory acclimation (Tjoelker *et al*. 2009; Reich *et al*. 2016), Type I acclimation has been observed more frequently in evergreen than deciduous species (Slot and Kitajima 2015). Additionally, the findings of this study fit into a generalized pattern of Type I acclimation playing a major role in the thermal acclimation of respiration in evergreen species (Crous *et al.* 2022). Therefore, despite the observed variation in the mechanism of acclimation, these findings support the growing consensus that most species demonstrate a generalized and predictable pattern of respiratory acclimation to temperature (Slot and Kitajima 2015; Heskel *et al*. 2016; Crous *et al.* 2022).

In summary, all four species and some populations demonstrated substantial evidence of respiratory acclimation to temperature, but each species demonstrated a different mechanism of acclimation. Additionally, none of the four species assessed demonstrated a significant relationship between $R_{realized}$ and T_{growth}. This finding suggests that the extent of acclimation in all four species was sufficient to maintain a near-homeostatic basal respiratory rate, despite

mechanistic differences in how the temperature response curve of respiration changed. Therefore, we reject the hypothesis that the extent of respiratory acclimation will vary among species from differing home climates. Future studies of respiratory acclimation may benefit from assessing how a temperature response curve changes shape and whether said mechanism is related to the climactic niche of a given species or population, in addition to assessing the overall extent of respiratory acclimation to temperature. Finally, as both temperature and photoperiod can independently affect physiological processes (Way and Montgomery 2015), additional research will be required to fully disentangle the roles of temperature and photoperiod on the observed seasonal responses of photosynthesis and respiration in southern pine species.

Species Show Significantly Different Sizes at Final Harvest

Significant differences at the species level were observed in the *RCD*, stem length, and dry mass of approximately two year old seedlings, as well as in the ratio of $A_{Net,25}$:R_{25}, although post-hoc tests revealed no significant comparisons in this variable. While the ratio of *A*:*R* is mathematically constrained at long timescales, short-term fluctuations in the ratio of *A*:*R* are possible in response to changes in the amount of carbon allocated to storage and growth (Van Oijen *et al.* 2010). In this study, the species-level variation in *RCD* at the time of final harvest corresponded closely to the nonsignificant, species-level trends in the mean values of the ratio of $A_{Net,25}$:R_{25}, with slash pine demonstrating the largest *RCD*, followed by longleaf and loblolly pine, then shortleaf pine. These findings reflect previously observed relationships between the temperature responses of physiological processes and growth rate. For example, previous work in red mangrove (*Rhizophora stylosa*) found similar trends in the temperature responses of *A*:*R* and the daily growth rates of height, diameter, and branch length (Akaji *et al.* 2019), while both A_{area} and R_{dark} were found to be correlated with relative growth rate for five boreal tree species across a range of growth temperatures (Tjoelker *et al.* 1998; Tjoelker *et al.* 1999). However, this trend was not observed for other metrics of seedling size, including stem length and total dry mass. While stem diameter at planting is considered the strongest indicator of future seedling growth potential (Grossnickle and MacDonald 2018), the connection between the temperature responses of $A_{Net,25}$:R_{25} and the long term growth potential of southern pine seedlings remains to be fully explored.

In summary, while the ratio of $A_{Net,25}$:R_{25} appears to explain some of the observed variation in final seedling size, other factors, such species-level variation in life-history traits, may also play a substantial role in determining seedling growth rate. Additionally, future research must be conducted to confirm that final sizes of the four assessed species were not constrained by their development within pots before these findings can be applied by foresters, nursery managers, or landowners. These findings contextualize the physiological findings of this study by providing a tangible illustration of the carbon balance between photosynthesis and respiration, though additional research will be required to fully elucidate the connection between photosynthetic and respiratory temperature responses and biomass production in southern pines.

Conclusions

Measurements of net photosynthesis and dark respiration were conducted for longleaf, loblolly, slash, and shortleaf pine grown in a common garden plot over a seasonal temperature gradient of 15°C. While significant evidence of respiratory adaptation was observed between the most southern and northern species, no evidence of photosynthetic adaptation was found at the species level. In contrast, all four species demonstrated at least partial respiratory and photosynthetic acclimation to increases in growth temperature. Finally, the method of respiratory and photosynthetic acclimation varied between all four species, and some mechanisms of respiratory and photosynthetic acclimation to temperature appeared to interact for a given species. These results emphasize that photosynthesis and respiration are complex, interrelated processes which may not be fully understood if studied in isolation. The potential adaptive and acclimatory responses of both photosynthesis and respiration must be considered in order to accurately predict the potential effects of climate warming on the growth and function of southern pine species.

References

Akaji Y, Inoue T, Tomimatsu H, Kawanishi A. 2019. Photosynthesis, respiration, and growth patterns of *Rhizophora stylosa* seedlings in relation to growth temperature. Trees 33:1041–1049.

Allakhverdiev SI, Vladimir D. Kreslavski VD, Klimov VV, Los DA, Carpentier R, Mohanty P. 2008. Heat stress: an overview of molecular responses in photosynthesis. Photosynth Res. 98:541–550.

Andersson I, Backlund A. 2008. Structure and function of Rubisco. Plant Physiol Biochem. 46:275-291.

Arias, PA, Bellouin N, Coppola E, Jones RG, Krinner G, Marotzke J, Naik V, Palmer MD, Plattner G-K, Rogelj J, Rojas M, Sillmann J, Storelvmo T, Thorne PW, Trewin B, Achuta Rao K, Adhikary B, Allan RP, Armour K, Bala G, Barimalala R, Berger S, Canadell JG, Cassou C, Cherchi A, Collins W, Collins WD, Connors SL, Corti S, Cruz F, Dentener FJ, Dereczynski C, Di Luca A, Diongue Niang A, Doblas-Reyes FJ, Dosio A, Douville H, Engelbrecht F, Eyring V, Fischer E, Forster P, Fox-Kemper B, Fuglestvedt JS, Fyfe JC, Gillett NP, Goldfarb L, Gorodetskaya I, Gutierrez JM, Hamdi R, Hawkins E, Hewitt HT, Hope P, Islam AS, Jones C, Kaufman DS, Kopp RE, Kosaka Y, Kossin J, Krakovska S, Lee J-Y, Li J, Mauritsen T, Maycock TK, Meinshausen M, Min S-K, Monteiro PMS, Ngo-Duc T, Otto F, Pinto I, Pirani A, Raghavan K, Ranasinghe R, Ruane AC, Ruiz L, Sallée J-B, Samset BH, Sathyendranath S, Seneviratne SI, Sörensson AA, Szopa S, Takayabu I, Tréguier A-M, van den Hurk B, Vautard R, von Schuckmann K, Zaehle S, Zhang X, Zickfeld K. 2021. Technical Summary. In *Climate Change 2021: The Physical Science Basis. Contribution of Working Group I to the Sixth Assessment Report of the Intergovernmental Panel on Climate Change* [Masson-Delmotte V, Zhai P, Pirani A, Connors SL, Péan C, Berger S, Caud N, Chen Y, Goldfarb L, Gomis MI, Huang M, Leitzell K, Lonnoy E, Matthews JBR, Maycock TK, Waterfield T, Yelekçi O, Yu R, Zhou B (eds.)]. Cambridge University Press, Cambridge, United Kingdom and New York, NY, USA, 33−144.

Aspinwall MJ, Jacob VK, Blackman CJ, Smith RA Tjoelker MG, Tissue DT. 2017a. The temperature response of leaf dark respiration in 15 provenances of *Eucalyptus grandis* grown in ambient and elevated CO_2. Funct. Plant. Biol. 44(11): 1075-1086.

Aspinwall MJ, Angelica Vårhammar A, Blackman CJ, Tjoelker MG, Ahrens C, Byrne M, Tissue DT, Rymer PD. 2017b. Adaptation and acclimation both influence photosynthetic and respiratory temperature responses in *Corymbia calophylla*. Tree Physiol. 37:1095–1112.

Atkin OK, Tjoelker MG. 2003. Thermal acclimation and the dynamic response of plant respiration to temperature. TRENDS in Plant Science 8(7): 343-351.

Bayer CropScience LP. 2019. Proline. [Label]. St. Louis, MO: Bayer CropScience.

Beer C, Reichstein M, Tomelleri E, Ciais P, Jung M, Carvalhais N, Rödenbeck C, Arain A, Baldocchi D, Bonan GB, Bondeau A, Cescatti A, Lasslop G, Lindroth A, Lomas M, Luyssaert S, Margolis H, Oleson KW, Roupsard O, Veenendaal E, Viovy N, Williams C, Woodward I, Papal D. 2010. Terrestrial Gross Carbon Dioxide Uptake: Global Distribution and Covariation with Climate. Nature 329: 834-838.

Berry J, Björkman O. 1980. Photosynthetic response and adaptation to temperature in higher plants. Ann. Rev. Plant Physiol. 31:491-543.

Björkman O, Badger M, Armond PA. 1978. Thermal acclimation of photosynthesis: effect of growth temperature on photosynthetic characteristics and components of the photosynthetic apparatus in *Nerium oleander*. Carnegie Inst. Washington Yearb. 77:262-82.

Bolstad PV, Reich P, Lee T. 2003. Rapid temperature acclimation of leaf respiration rates in *Quercus alba* and *Quercus rubra*. Tree Physiol. 23:969–976.

Bukenhofer GA, Neal JC, Montague WG. 1994. Shortleaf pine/bluestem grass ecosystem and red-cockaded woodpeckers. JAAS 48:243-245.

Campbell Scientific, Inc. 2020. HS2 and HS2P. [Manual]. Logan, Utah: Campbell Scientific, Inc.

Collier RJ, Baumgard LH, Zimbelman RB, Xiao Y. 2019. Heat stress: physiology of acclimation and adaptation. Animal Frontiers 9(1):12–19.

Crous KY, Uddling J, De Kauwe MG. 2022. Temperature responses of photosynthesis and respiration in evergreen trees from boreal to tropical latitudes. New Phytol. [22 pages].

Das J. 2006. The role of mitochondrial respiration in physiological and evolutionary adaptation. BioEssays 28:890–901.

Dillaway DN, Kruger EL. 2010. Thermal acclimation of photosynthesis: a comparison of boreal and temperate tree species along a latitudinal transect. Plant Cell Environ. 33:888–899.

Dusenge ME, Duarte AG, Way DA. 2019. Plant carbon metabolism and climate change: elevated CO_2 and temperature impacts on photosynthesis, photorespiration and respiration. New Phytol. 221:32–49.

Duursma RA. 2015. Plantecophys - An R Package for Analysing and Modelling Leaf Gas Exchange Data. PLOS One 10(11): e0143346.

Elzhov TV, Mullen KM, Spiess A-N, Bolker B. 2023. minpack.lm: R Interface to the Levenberg-Marquardt Nonlinear Least-Squares Algorithm Found in MINPACK, Plus Support for Bounds. R package version 1.2-3.

Evergreen. 2022. Evergreen 1 Cubic Foot Top Soil. [Website]. Mooresville, NC: Lowes.

Fan Y, Zhong Z, Zhang X. 2011. Determination of photosynthetic parameters V_{cmax} and J_{max} for a C_3 plant (spring hulless barley) at two altitudes on the Tibetan Plateau. Agric For Meteorol. 151:1481–1487.

Farquhar GD, von Caemmerer S, Berry JA. 1980. A biochemical model of photosynthetic CO_2 assimilation in leaves of C_3 species. Planta 149:78-90.

Fernández-Marín B, Gulías J, Figueroa CM, Iñiguez C, Clemente-Moreno MJ, Nunes-Nesi A, Fernie AR, Cavieres LA, Bravo LA, García-Plazaola JI, Gago J. 2020. How do vascular plants perform photosynthesis in extreme environments? An integrative ecophysiological and biochemical story. The Plant Journal 101:979–1000.

Flexas J, Barbour MM, Brendel O, Cabrera HM, Carriquí M, Díaz-Espejo A, Douthe C, Dreyer E, Ferriog JP, Gago J, Gallé A, Galmés J, Kodama N, Medranoa H, Niinemets Ü, Peguero-Pina JJ, Pou A, Ribas-Carbó M, Tomás M, Tosens T, Warren CR. 2012. Mesophyll diffusion conductance to CO2: An unappreciated central player in photosynthesis. Plant Science 193–194:70–84.

Fox J, Weisberg S. 2019. An R Companion to Applied Regression, Third Edition. Thousand Oaks CA: Sage.

Ghannoum O, Way DA. 2011. On the role of ecological adaptation and geographic distribution in the response of trees to climate change. Tree Physiol. 31:1273–1276.

Grossnickle SC, MacDonald JE. 2018. Why seedlings grow: influence of plant attributes. New Forests 49:1–34.
Guschina IA, Harwood JL. 2006. Mechanisms of temperature adaptation in poikilotherms. FEBS Letters 580:5477–5483.
Harris NL, Gibbs DA, Baccini A, Birdsey RA, de Bruin S, Farina M, Fatoyinbo L, Hansen MC, Herold M, Houghton RA, Potapov PV, Suarez DR, Roman-Cuesta RM, Saatchi SS, Slay CM, Turubanova SA, Tyukavina A. 2021. Global maps of twenty-first century forest carbon fluxes. Nature Climate Change 11:234–240.
Hermida-Carrera C, Kapralov MV, Galmés J. 2016. Rubisco catalytic properties and temperature response in crops. Plant Physiol. 171:2549–2561.
Heskel MA, O'Sullivan OS, Reich PB, Tjoelker MG, Weerasinghe LK, Penillarda A, Egerton JJG, Creek D, Bloomfield KJ, Xiang J, Sinca F, Stangl ZR, Martinez-de la Torrej A, Griffin KL, Huntingford C, Hurry V, Meira P, Turnbullo MH, Atkin OK. 2016. Convergence in the temperature response of leaf respiration across biomes and plant functional types. PNAS 113(14):3832–3837.
Hikosaka K, Ishikawa K, Borjigidai A, Muller O, Onoda Y. 2005. Temperature acclimation of photosynthesis: mechanisms involved in the changes in temperature dependence of photosynthetic rate. J Exp Bot. 57(2):291–302.
Hüve K, Bichele I, Tobias M, Niinemets Ü. 2006. Heat sensitivity of photosynthetic electron transport varies during the day due to changes in sugars and osmotic potential. Plant Cell Environ. 29:212–228.
Jolley GJ, Khalaf C, Michaud GL, Belleville D. 2020. The economic contribution of logging, forestry, pulp & paper mills, and paper products: A 50-state analysis. For. Pol. Econ. 115:102140. [20 pages].
Kattge J, Knorr W. 2007. Temperature acclimation in a biochemical model of photosynthesis: a reanalysis of data from 36 species. Plant Cell Environ. 30:1176-1190.
Kirilenko AP, Sedjo RA. 2007. Climate change impacts on forestry. PNAS 50(104):19697–19702.
Kositsup B, Montpied P, Kasemsap P, Thaler P, Améglio T, Dreyer E. 2009. Photosynthetic capacity and temperature responses of photosynthesis of rubber trees (*Hevea brasiliensis* Müll. Arg.) acclimate to changes in ambient temperatures. Trees 23:357–365.
Kuhn M, Wing J, Weston S, Williams A, Keefer C, Engelhardt A, Cooper T, Mayer Z, Kenkel B, R Core Team, Benesty M, Lescarbeau R, Ziem A, Scrucca L, Tang Y, Candan C, Hunt T. 2023. caret: Classification and Regression Training. R package version 6.0-94.
Kumarathunge DP, Medlyn BE, Drake JE, Tjoelker MG, Aspinwall MJ, Battaglia M, Cano FJ, Carter KR, Cavaleri MA, Cernusak LA, Chambers JQ, Crous KY, De Kauwe MG, Dillaway DN, Dreyer E, Ellsworth DS, Ghannoum O, Han Q, Hikosaka K, Jensen AM, Kelly JWG, Eric L. Kruger EL, Lina M. Mercado LM, Yusuke Onoda Y, Reich PB, Rogers A, Slot M, Smith NG, Tarvainen L, Tissue DT, Togashi HF, Tribuzy ES, Uddling J, Vårhammar A, Wallin G, Warren JM, Way DA. 2019. Acclimation and adaptation components of the temperature dependence of plant photosynthesis at the global scale. New Phytol. 222:768–784.
Lenth RV, Bolker B, Buerkner P, Giné-Vázquez I, Herve M, Jung M, Love J, Miguez F, Riebl H, Singmann H. 2023. emmeans: Estimated Marginal Means, aka Least-Squares Means. R package version 1.8.6.

Lemon J, Bolker B, Oom S, Klein E, Rowlingson B, Wickham H, Tyagi A, Eterradossi O, Grothendieck G, Toews M, Kane J, Turner R, Carl Witthoft C, Stander J, Petzoldt T, Duursma R, Biancotto E, Levy O, Dutang C, Solymos P, Engelmann R, Hecker M, Steinbeck F, Borchers H, Singmann H, Toal T, Ogle D, Baral D, Groemping U, Venables B. 2009. plotrix: Various Plotting Functions. R package version 3.8-2.

Lombardozzi DL, Bonan GB, Smith NG, Dukes JS, Fisher RA. 2015. Temperature acclimation of photosynthesis and respiration: A key uncertainty in the carbon cycle-climate feedback. Geophys. Res. Lett. 42: 8624–8631.

Medlyn BE, Loustau D, Delzon S. 2002. Temperature response of parameters of a biochemically based model of photosynthesis. I. Seasonal changes in mature maritime pine (*Pinus pinaster* Ait.). Plant Cell Environ. 25:1155–1165.

Millar AH, Whelan J, Soole KL, Day DA. 2011. Organization and Regulation of Mitochondrial Respiration in Plants. Annu. Rev. Plant Biol. 62: 79–104.

Mohammed A-R, Tarpley L. 2009. Impact of high nighttime temperature on respiration, membrane stability, antioxidant capacity, and yield of rice plants. Crop Sci. 49:313–322.

Niinemets Ü, Díaz-Espejo A, Flexas J, Galmé J, Warren CR. 2009. Role of mesophyll diffusion conductance in constraining potential photosynthetic productivity in the field. J. Exp. Bot. 60(8):2249–2270.

Oleksyn J, Modrzyński J, Tjoelker MG, Żytkowiak R, Reich PB, Karolewski P. 1998. Growth and physiology of *Picea abies* populations from elevational transects: common garden evidence for altitudinal ecotypes and cold adaptation. Funct. Ecol. 12:573–590.

Onoda Y, Hikosaka K, Hirose T. 2005. The balance between RuBP carboxylation and RuBP regeneration: a mechanism underlying the interspecific variation in acclimation of photosynthesis to seasonal change in temperature. Funct. Plant Biol. 32: 903–910.

O'Sullivan OS, Lasantha KW, Weerasinghe K, Evans JR, Egerton JJG, Tjoelker MG, Atkin OK. 2013. High-resolution temperature responses of leaf respiration in snow gum (*Eucalyptus pauciflora*) reveal high-temperature limits to respiratory function. Plant Cell Environ. 36:1268–1284.

Pinheiro J, Bates D, R Core Team. 2023. nlme: Linear and Nonlinear Mixed Effects Models. R package version 3.1-162.

Quan X, Wang C. 2018. Acclimation and adaptation of leaf photosynthesis, respiration and phenology to climate change: A 30-year *Larix gmelinii* common-garden experiment. For. Ecol. Manag. 411:166-175.

R Core Team. 2022. R: A language and environment for statistical computing. R Foundation for Statistical Computing, Vienna, Austria.

Reich PB, Oleksyn J, Tjoelker MG. 1996. Needle respiration and nitrogen concentration in Scots Pine populations from a broad latitudinal range: a common garden test with field-grown trees. Funct. Ecol. 10:768-776.

Reich PB, Sendall KM, Stefanski A, Wei X, Rich RL, Montgomery RA. 2016. Boreal and temperate trees show strong acclimation of respiration to warming. Nature 531:633-636.

Ripley B, Venables B, Bates DM, Hornik K, Gebhardt A, Firth D. 2023. MASS: Support Functions and Datasets for Venables and Ripley's MASS. R package version 7.3-58.3.

Rogers A, Medlyn BE, Dukes JS, Bonan G, von Caemmerer S, Dietze MC, Kattge J, Leakey ADB, Mercado LM, Niinemets Ü, Prentice C, Serbin SP, Sitch S, Way DA, Zaehle S. 2017. A roadmap for improving the representation of photosynthesis in Earth system models. New Phytol. 213:22–42.

Sage, RF, Way DA, Kubien DS. 2008. Rubisco, Rubisco activase, and global climate change. J Exp Botany 59(7):1581–159.
Salvucci ME, Osteryoung KW, Crafts-Brandner SJ, Vierling E. 2001. Exceptional sensitivity of Rubisco activase to thermal denaturation in vitro and in vivo. Plant Physiol. 127:1053–1064.
Samuelson LJ, Stokes TA, Johnsen KH. 2012. Ecophysiological comparison of 50-year-old longleaf pine, slash pine, and loblolly pine. For. Ecol. Manag. 274:108-115.
Scafaro AP, Posch BC, Evans JR, Farquhar GD, Atkin OK. 2023. Rubisco deactivation and chloroplast electron transport rates co-limit photosynthesis above optimal leaf temperature in terrestrial plants. Nature Communications 14:2820.
Schultz RP. 1999. Loblolly – the pine for the twenty-first century. New Forests 17:71–88.
Sharkey TD, Zhang R. 2010. High temperature effects on electron and proton circuits of photosynthesis. J Int Plant Biology 52(8):712–722.
Silim SN, Ryan N, Kubien DS. 2010. Temperature responses of photosynthesis and respiration in *Populus balsamifera* L.: acclimation versus adaptation. Photosynth. Res. 104:19–30.
Slayter RO, Ferrar PJ. 1977. Altitudinal variation in the photosynthetic characteristics of snow gum, Eucalyptus pauciflora Sieb. ex Spreng. II.* Effects of growth temperature under controlled conditions. Aust J Plant Physiol. 4:289-99.
Slot M, Kitajima K. 2015. General patterns of acclimation of leaf respiration to elevated temperatures across biomes and plant types. Oecologia 177:885–900.
Stirbent A, Lazár D, Guo Y, Govindjee G. 2019. Photosynthesis: basics, history and modelling. Ann. Bot. 126:511–537.
Stuewe and Sons, Inc. 2023. TP915R – 9 X 15.5″ TREEPOT. [Website]. Tangent, OR: Stuewe and Sons, Inc.
Teskey RO, Will RE. 1999. Acclimation of loblolly pine (*Pinus taeda*) seedlings to high temperatures. Tree Physiol. 19:519-525.
Tiwari R, Gloor E, da Cruz WJA, Marimon BS, Marimon-Junior BH, Reis SM, de Souza IA, Krause HG, Slot M, Winter K, Ashley D, Béu RG, Bores CS, Da Cunha M, Fauset S, Marques EQ, Mendonça NG, Mendonça NG, Noleto PT, de Oliveira CHL, Oliveira MA, Pireda S, dos Santos Prestes NCC, Santos DM, Santos EB, da Silva ELS, de Souza IA, de Souza LJ, Vitória AP, Foyer CH, Galbraith D. 2020. Photosynthetic quantum efficiency in south-eastern Amazonian trees may be already affected by climate change. Plant Cell Environ. 44:2428–2439.
Tjoelker MG, Oleksyn J, Reich PB. 1998. Seedlings of five boreal tree species differ in acclimation of net photosynthesis to elevated CO_2 and temperature. Tree Phys. 18:715-726.
Tjoelker MG, Oleksyn J, Reich PB. 1999. Acclimation of respiration to temperature and CO_2 in seedlings of boreal tree species in relation to plant size and relative growth rate. Glob. Change Biol. 49:679-691.
Tjoelker MG, Oleksyn J, Lorenc-Plucinska G, Reich PB. 2009. Acclimation of respiratory temperature responses in northern and southern populations of *Pinus banksiana*. New Phytol. 181: 218–229.
Urban J, Ingwers M, McGuire MA, Teskey RO. 2017. Stomatal conductance increases with rising temperature. Plant Signaling and Behavior 12(8). [3 pages].

Van Lear DH, Carroll WD, Kapeluck PR, Johnson R. 2005. History and restoration of the longleaf pine-grassland ecosystem: Implications for species at risk. For. Ecol. Manag. 211:150–165.
van Mantgem PJ, Stephenson NL, Byrne JC, Daniels LD, Franklin JF, Fulé PZ, Harmon ME, Larson AJ, Smith JM, Taylor AH, Veblen TT. 2009. Widespread increase of tree mortality rates in the western United States. Science 323:521-524.
Van Oijen M, Schapendonk A, Högland M. 2010. On the relative magnitudes of photosynthesis, respiration, growth and carbon storage in vegetation. Ann. Bot. 105:793 –797.
Wang B, Cai W, Li J, Wan Y, Li Y, Guo C, Wilkes A, You S, Qin X, Gao Q, Liu K. 2020. Leaf photosynthesis and stomatal conductance acclimate to elevated [CO_2] and temperature thus increasing dry matter productivity in a double rice cropping system. Field Crops Res. 248:107735. [11 pages].
Way DA, Yamori W. 2013. Thermal acclimation of photosynthesis: on the importance of adjusting our definitions and accounting for thermal acclimation of respiration. Photosynth Res. 119:89–100.
Way DA, Holly C, Bruhn D, Ball MC, Atkin OK. 2015. Diurnal and seasonal variation in light and dark respiration in field-grown *Eucalyptus pauciflora*. Tree Physiol. 35:840–849.
Way DA, Montgomery RA. 2015. Photoperiod constraints on tree phenology, performance and migration in a warming world. Plant Cell Environ. 38:1725–1736.
Wei X, Sendall KM, Stefanski A, Zhao C, Hou J, Rich RL, Montgomery RA, Reich PB. 2016. Consistent leaf respiratory response to experimental warming of three North American deciduous trees: a comparison across seasons, years, habitats and sites. Tree Physiol. 37:285–300.
Wells OO, Wakeley PC. 1970. Variation in shortleaf pine from several geographic sources. Forest Sci. 16:415-423.
Williams DA, Wang Y, Borchetta M, Gaines MS. 2007. Genetic diversity and spatial structure of a keystone species in fragmented pine rockland habitat. Biol. Conserv. 138:256–268.
Winston Weaver Co., Inc. 2022. All-Purpose Plant Food. [Website]. Winston Salem, NC: Winston Weaver Co., Inc.
Yamori W, Noguchi K, Terashima I. 2005. Temperature acclimation of photosynthesis in spinach leaves: analyses of photosynthetic components and temperature dependencies of photosynthetic partial reactions. Plant Cell Environ. 28:536–547.
Yamori W, Hikosaka K, Way DA. 2014. Temperature response of photosynthesis in C3, C4, and CAM plants: temperature acclimation and temperature adaptation. Photosynth Res. 119:101–117.
Yang JT, Preiser AL, Li Z, Weise SE, Sharkey TD. 2016. Triose phosphate use limitation of photosynthesis: short-term and long-term effects. Planta 243:687–698.
Zhu L, Bloomfield KJ, Asao S, Tjoelker MG, Egerton JJG, Hayes L, Weerasinghe LK, Creek D, Griffin KL, Hurry V, Liddell M, Meir P, Turnbull MH, Atkin OK. 2021. Acclimation of leaf respiration temperature responses across thermally contrasting biomes. New Phytol. 229:1312–1325.